Supporting Information

Remote-control of the enantiomeric supramolecular recognition mediated by chiral azobenzenes bound to human serum albumin

Marco Deiana,[a] Ziemowit Pokladek,[a,b] Marta Dudek,[a,b] Sebastian G. Mucha,[a] Leszek M. Mazur,[a] Krzysztof Pawlik,[c] Piotr Mlynarz,[b] Marek Samoc,[a] Katarzyna Matczyszyn[a]*

[a]Advanced Materials Engineering and Modelling Group, Faculty of Chemistry, Wroclaw University of Science and Technology, Wyb. Wyspianskiego 27, 50-370 Wroclaw, Poland

[b]Department of Bioorganic Chemistry, Faculty of Chemistry, Wroclaw University of Science and Technology, Wyb. Wyspianskiego 27, 50-370 Wroclaw, Poland

[c]Ludwik Hirszfeld Institute of Immunology and Experimental Therapy, Polish Academy of Sciences, Rudolfa Weigla 12, 53-114 Wroclaw, Poland

Table of Contents:

Synthesis

NMR-spectra were recorded on a Bruker Avance^{TM} 600 MHz spectrometer. Mass spectra were conducted with a WATERS LCT Premier XE mass spectrometer (ESI). Unless otherwise noted, all reactions were carried out under normal conditions. Materials and solvents obtained from commercial suppliers were used without further purification.

Synthesis of 1

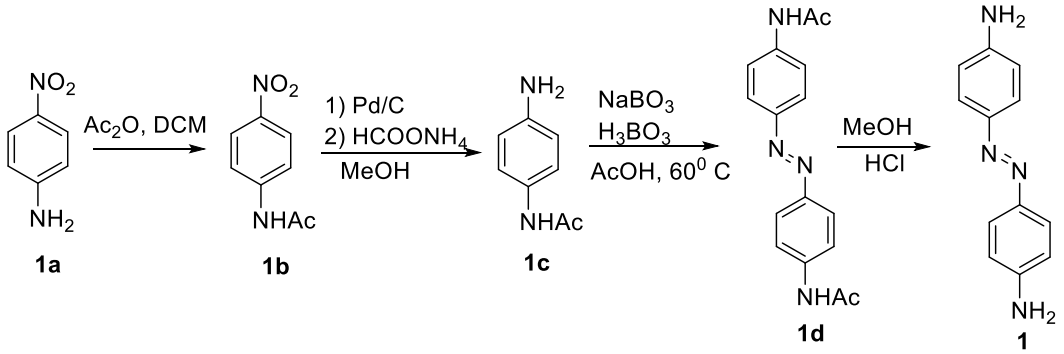

N-(4-nitrophenyl)acetamide (1b). To a solution of 4-nitroaniline (0.5 g, 3.6 mmol, 1 equiv.) in dichloromethane (30 mL), acetic anhydride (0.44 g, 4.3 mmol, 1.2 ek) was added at room temperature. The mixture was stirred overnight, diluted with saturated solution of sodium carbonate and then DCM was added. The organic phase was dried over $MgSO_4$, filtered, and concentrated under reduced pressure to give **1b** as a greenish solid (0.58 g, 98 %).

^{1}H NMR (601 MHz, DMSO-d_6) δ:

10.54 (s, 1H), 8.20 (d, $^3J_{H,H}$ = 9.3 Hz, 2H), 7.82 (d, $^3J_{H,H}$ = 9.3 Hz, 2H), 2.12 (s, 3H).

HRMS m/z (ESI): calcd for $C_8H_8N_2O_3$: $[M+H]^+$,

Required: 181.0613, found: 181.0620

***N*-(4-aminophenyl)acetamide (1c).** To a solution of **1b** (1.12 g, 6.2 mmol, 1 equiv.) in MeOH (30 mL), under argon atmosphere, at 0^{o}C, 10% Pd/C (0.311 g) and ammonium formate (1.8 g, 4.6 mmol, 1 equiv.) were added. After 1 h, the reaction mixture was filtered through short plug of Celite, dried over MgSO4, filtered, and concentrated under reduced pressure to give **1c** as a pale pink powder (0.93 g, quantitative).

^{1}H NMR (601 MHz, DMSO-d_6) δ:

9.46 (s, 1H), 7.18 (d, $^3J_{H,H}$ = 8.7 Hz, 2H), 6.47 (d, $^3J_{H,H}$ = 8.7 Hz, 2H), 4.80 (s, 2H), 1.23 (s, 3H).

HRMS m/z (ESI): calcd for: $C_8H_{10}N_2O$: $[M+H]^+$,
Required: 151.0871, found: 151.0870

***(E)-N,N'*-(diazene-1,2-diylbis(4,1-phenylene))diacetamide (1d).** To a solution of **1c** (2.42 g, 16 mmol, 1 equiv.) in glacial acetic acid (40 mL), sodium perborate tetrahydrate (3.3 g, 021 mmol, 1.3 equiv.) and boric acid (0.83 g, 13 mmol 0.8 equiv.) were added and the solution was heated under reflux for 7 h. The mixture was cooled to room temperature and the formed solid was filtered, washed with water and dried under vacuum. The **1d** was obtained as a green - yellow powder (1.52 g, 32 %).

^{1}H NMR (601 MHz, MeOD) δ:
10.21 (s, 2H), 7.77 (d, $^3J_{H,H}$ = 8.9 Hz, 4H), 7.73 (d, $^3J_{H,H}$ = 8.9 Hz, 4H), 2.04 (s, 6H).
HRMS m/z (ESI): calcd for: $C_{16}H_{16}N_4O_2$: $[M+H]^+$,
Required: 297.1352, found: 297.1358

(*E*)-4,4'-(diazene-1,2-diyl)dianiline (1). To a solution of **1d** (1.4 g, 4.7 mmol, 1 equiv.) in MeOH, 20 mL of 6M HCl were added and heated at 75^{o}C for 6.5 h. MeOH was evaporated and the mixture was slowly neutralized by the addition of 2M NaOH. The formed solid was filtered and washed with water and dried. The **1** was obtained as a green-brown powder (0.8 g, 80 %).

^{1}H NMR (601 MHz, Methanol -d) δ:
7.48 (d, $^3J_{H,H}$ = 8.7 Hz, 4H), 6.59 (d, $^3J_{H,H}$ = 8.7 Hz, 4H), 5.69 (s, 4H).
HRMS m/z (ESI): calcd for: $C_{12}H_{12}N_4$: $[M+H]^+$,
Required: 213.1140, found: 213.1141

Synthesis of 2 and 3

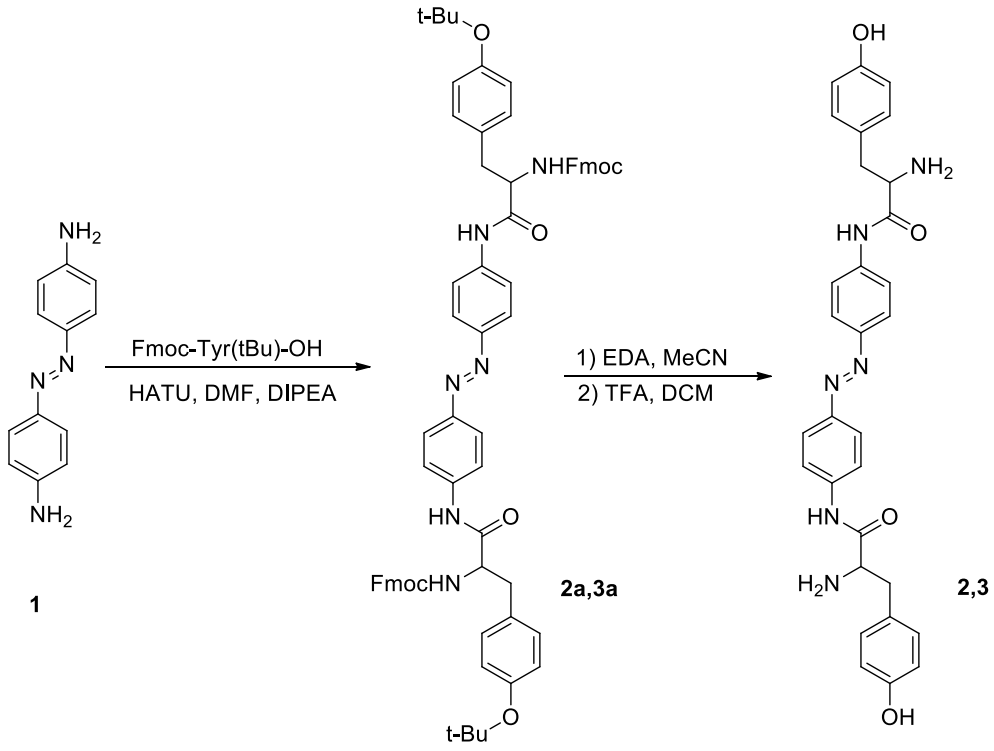

(E)-N,N'-(diazene-1,2-diylbis(4,1-phenylene))bis(2-amino-3-(4-hydroxyphenyl)propana mide) (2-L, 3-D Fmoc-Tyr(tBu)-OH). To a solution of Fmoc-Tyr(tBu)-OH (D for **2** and L for **3**) (0.43 g, 0.93 mmol, 2.2 equiv.) in DMF (10 mL) , DIPEA (0.24 g, 1.9 mmol, 4.4 equiv.) and HATU (0.35 g, 0.93 mmol, 2.2 equiv.) were added. After 30 s (E)-4,4'-(diazene-1,2-diyl)dianiline (90 mg, 0.42 mmol, 1 equiv.) was added. The reaction mixture was stirred for 6 h at room temperature. Solvent was removed under reduced pressure, then EtOAc was added and the solution was passed through short plug of silica, and washed with EtOAc (30 mL). Without further purification - F-moc was removed by adding to crude (0.4 g) **2a (or 3a)**, ethylenediamine (eda) (0.8 mL) in MeCN (0.8 mL). The mixture was stirred for 2 h and concentrated under reduced pressure. The obtained solid was dissolved in DCM (20 mL) and TFA (1 mL) was added; the reaction mixture was stirred overnight. Solvent was removed under vacuum and crude was purified by HPLC with gradient from water to water/MeCN (1/1) in 20 minutes. **2** and **3** were obtained as red powders (**2**: 79 mg, 32% **3**: 83 mg, 36%).

Spectral data for **2**:

^{1}H NMR (601 MHz, D_2O) δ:

7.74 (d, *J* = 8.8 Hz, 2H), 7.45 (d, *J* = 9.0 Hz, 2H), 7.12 (d, *J* = 8.3 Hz, 2H), 6.82 (d, *J* = 8.1 Hz, 2H), 4.27 (t, *J* = 7.3 Hz, 1H), 3.18 (dd, *J* = 14.1, 6.9 Hz, 1H), 3.11 (dd, *J* = 14.1, 7.8 Hz, 1H).

^{13}C NMR (600 MHz, D_2O) δ:
167.69, 155.15, 149.16, 138.82, 130.84, 125.34, 123.45, 121.65, 115.83, 55.16, 36.25.

HRMS m/z (ESI): calcd for: $C_{39}H_{27}N_9O_3$: $[M+H]^+$,

Required: 539.2407, found: 539.2402

Spectral data for **3**:

^{1}H NMR (601 MHz, D_2O) δ:

7.85 (d, *J* = 8.8 Hz, 4H), 7.53 (d, *J* = 8.8 Hz, 4H), 7.19 (d, *J* = 8.5 Hz, 4H), 6.88 (d, *J* = 8.5 Hz, 4H), 4.33 (t, *J* = 7.5 Hz, 2H), 3.28 (dd, *J* = 14.1, 6.7 Hz, 2H), 3.19 (dd, *J* = 14.0, 8.1 Hz, 2H).

^{13}C NMR (600 MHz, D_2O) δ:

167.76 , 155.18 , 149.29 , 138.84 , 130.88 , 125.41 , 123.47 , 121.76 , 115.87 , 55.20 , 36.28 .

HRMS m/z (ESI): calcd for: $C_{30}H_{30}N_6O_4$: $[M+H]^+$,

Required: 539.2407, found: 539.2418

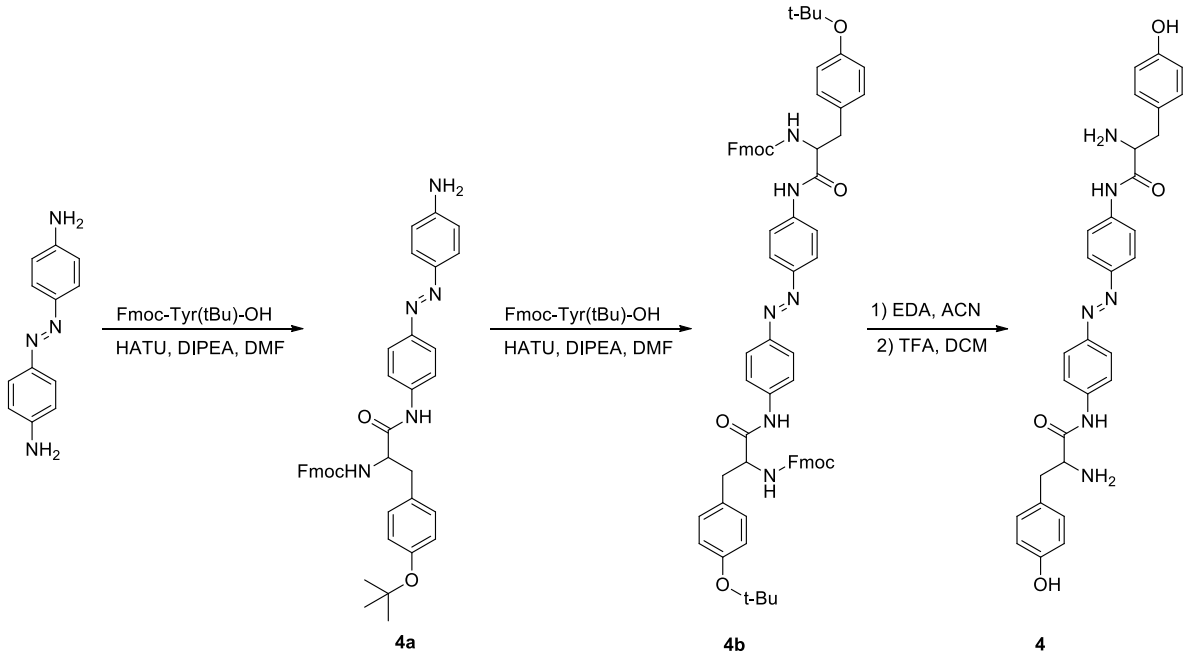

(*E*)-(9H-fluoren-9-yl)methyl(1-((4-((4-aminophenyl)diazenyl)amino)-3-(4-(*tert*-butoxy)phenyl)-1-oxopropan-2-yl)carbomate (4a). To a solution of L-tyrosine (0.28 g, 0.6mmol, 1.1 equiv.) in DMF (10 mL), DIPEA (0.15 g, 1.2 mmol, 2.2 equiv.), HATU (0.23 g, 0.6 mmol, 1.1 equiv.) were added. After 30 s (E)-4,4'-(diazene-1,2-diyl)dianiline (0.12 g, 0.54 mmol, 1

equiv.) was added and the reaction mixture was stirred overnight at room temperature. The solvent was removed under reduced pressure, the reside was diluted with water (30 mL) and extracted with diethyl ether (50 mL). Combined organic phases were dried over $MgSO_4$, filtered, and concentrated under reduced pressure. The crude **4a** was purified by column chromatography on SiO_2 using gradient from DCM to EtOAc. **4a** was obtained as an orange powder (0.19 g, 53 %).

^{1}H NMR (601 MHz, $CDCl_3$) δ:

7.87 (t, *J* = 8.6, Hz, 2H), 7.77 (d, *J* = 7.5 Hz, 2H), 7.61 – 7.46 (m, 5H), 7.40 (t, *J* = 7.4 Hz, 2H), 7.30 (m, 3H), 7.22 (d, *J* = 8.5 Hz, 1H), 6.94 (d, *J* = 7.9 Hz, 12),4.47 (m, 3H), 4.22 (t, *J* = 6.7 Hz, 2H), 4.13 (d, *J* = 7.2 Hz, 1H), 4.11 (d, *J* = 7.2 Hz, 1H), 1.32 (s, 9H).

HRMS: $C_{40}H_{39}N_5O_4$: $[M+H]^+$,

Required: 654.3080, found: 654.3067

(E)-N,N'-(diazene-1,2-diylbis(4,1-phenylene))bis(2-amino-3-(4-hydroxyphenyl)propanamide) (4). To a solution of D-tyrosine (0.16 g, 0.34mmol, 1.2 equiv.) in DMF (10 mL), DIPEA (0.09 g, 0.69 mmol, 2.4 eq) and HATU (0.13 g, 0.34 mmol, 1.2 equiv.) were added. After 30 s **4a** (0.19 g, 0.29 mmol, 1 equiv.) was added and reaction mixture was stirred overnight at room temperature. Without further purification - F-moc was removed by adding to **4b** (0.1 g,) ethylenediamine (0.4 mL) solution in MeCN (0.4 mL). The mixture was stirred for 2 h and concentrated under reduced pressure. Crude was dissolved in DCM (20 mL), trifluoroacetic acid (1 mL) was added and the mixture was stirred overnight. The reaction mixture was concentrated under reduced pressure and purified by HPLC with gradient from water to water/MeCN (1/1) in 20 minutes. **4** was obtained as a red powder (30 mg, 61 %).

^{1}H NMR (601 MHz, D_2O) δ:

7.85 (d, *J* = 8.8 Hz, 4H), 7.51 (d, *J* = 8.8 Hz, 4H), 7.18 (d, *J* = 8.5 Hz, 4H), 6.86 (d, *J* = 8.5 Hz, 4H), 4.31 (t, *J* = 7.7 Hz, 2H), 3.27 (dd, *J* = 14.0, 6.6 Hz, 2H), 3.17 (dd, *J* = 14.0, 8.2 Hz, 2H).

^{13}C NMR (600 MHz, D_2O) δ:

167.75, 155.15, 149.31, 138.79, 130.85, 125.39, 123.45, 121.78, 115.83, 55.18, 36.25.

HRMS: $C_{30}H_{30}N_6O_4$: $[M+H]^+$,

Required: 539.2407, found: 539.2410

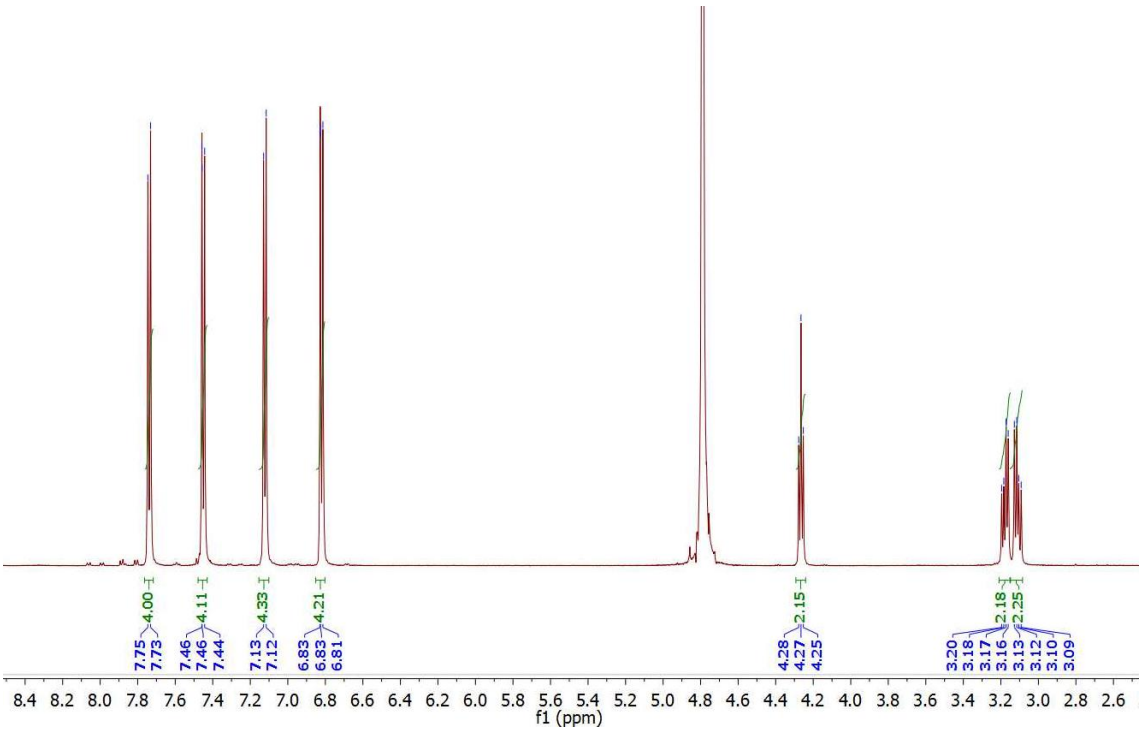

Figure S1. ^{1}H-NMR spectra of **2** (**Azo-DD-Tyr**).

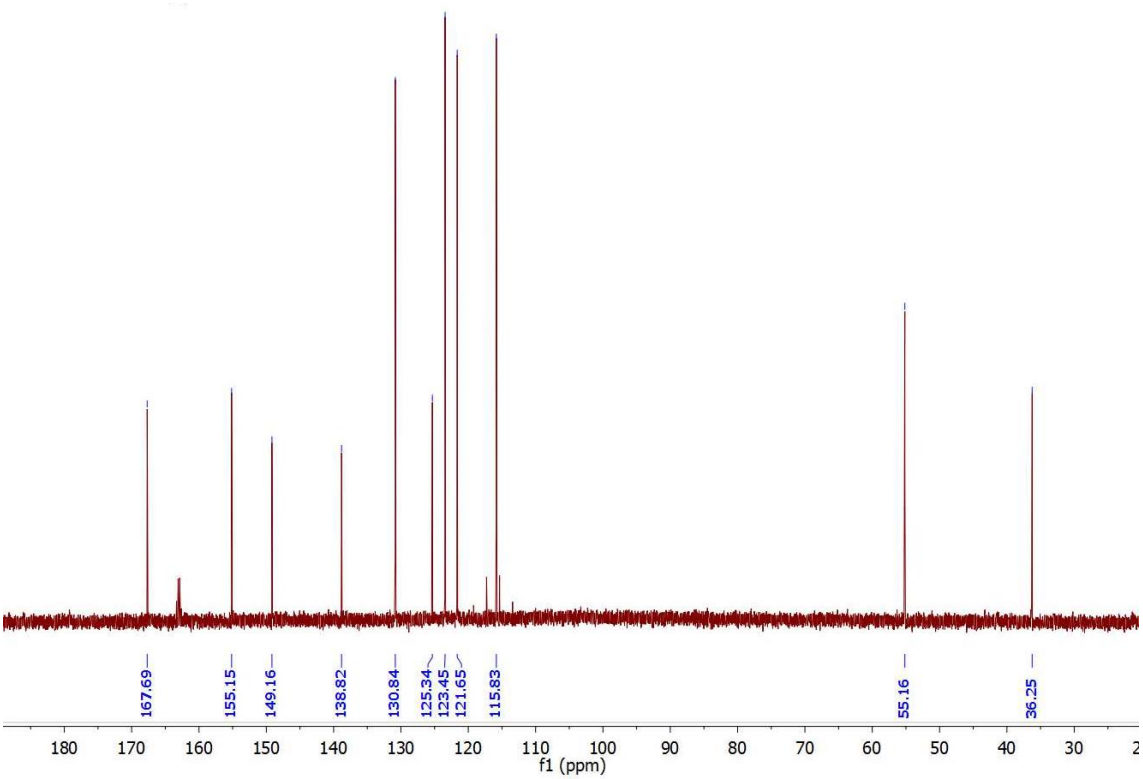

Figure S2. ^{13}C-NMR spectra of **2** (**Azo-DD-Tyr**).

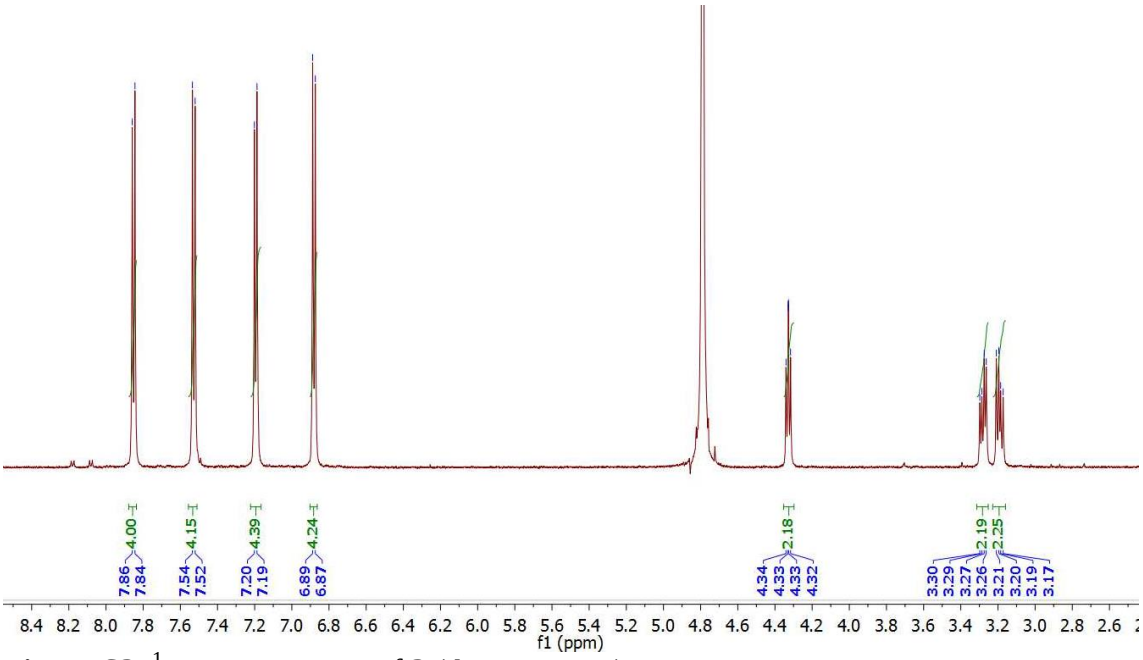

Figure S3. ^{1}H-NMR spectra of **3** (**Azo-LL-Tyr**).

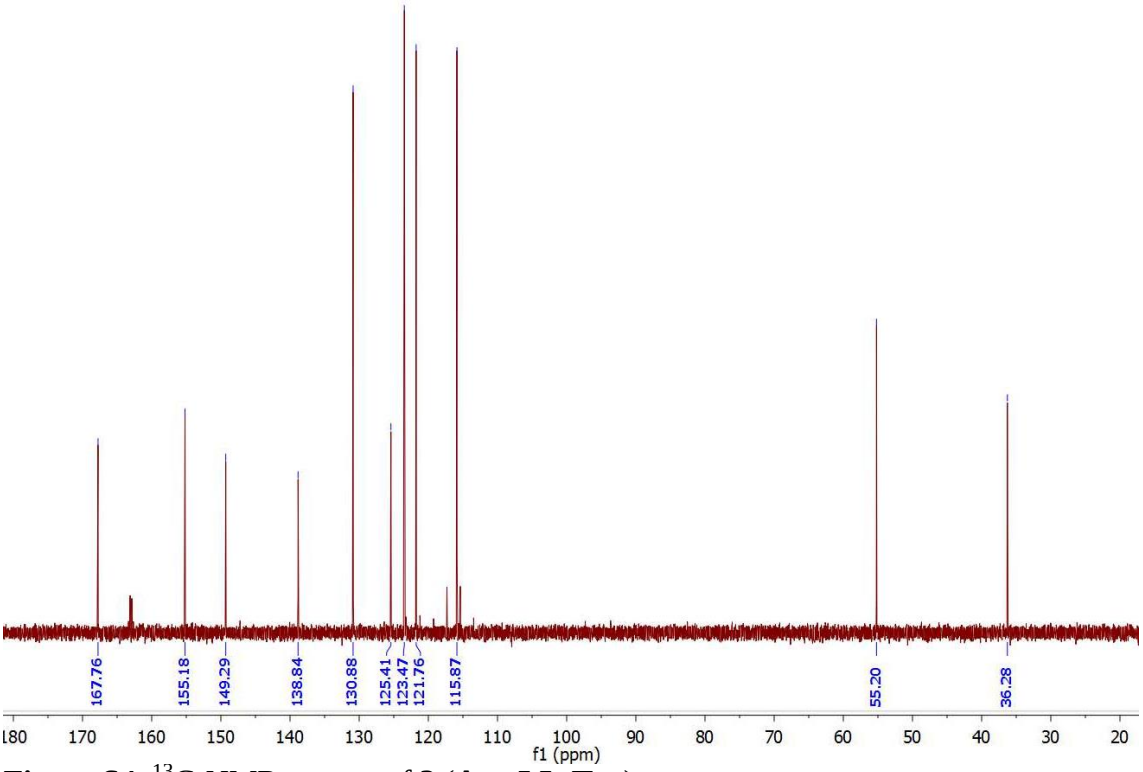

Figure S4. ^{13}C-NMR spectra of **3** (**Azo-LL-Tyr**).

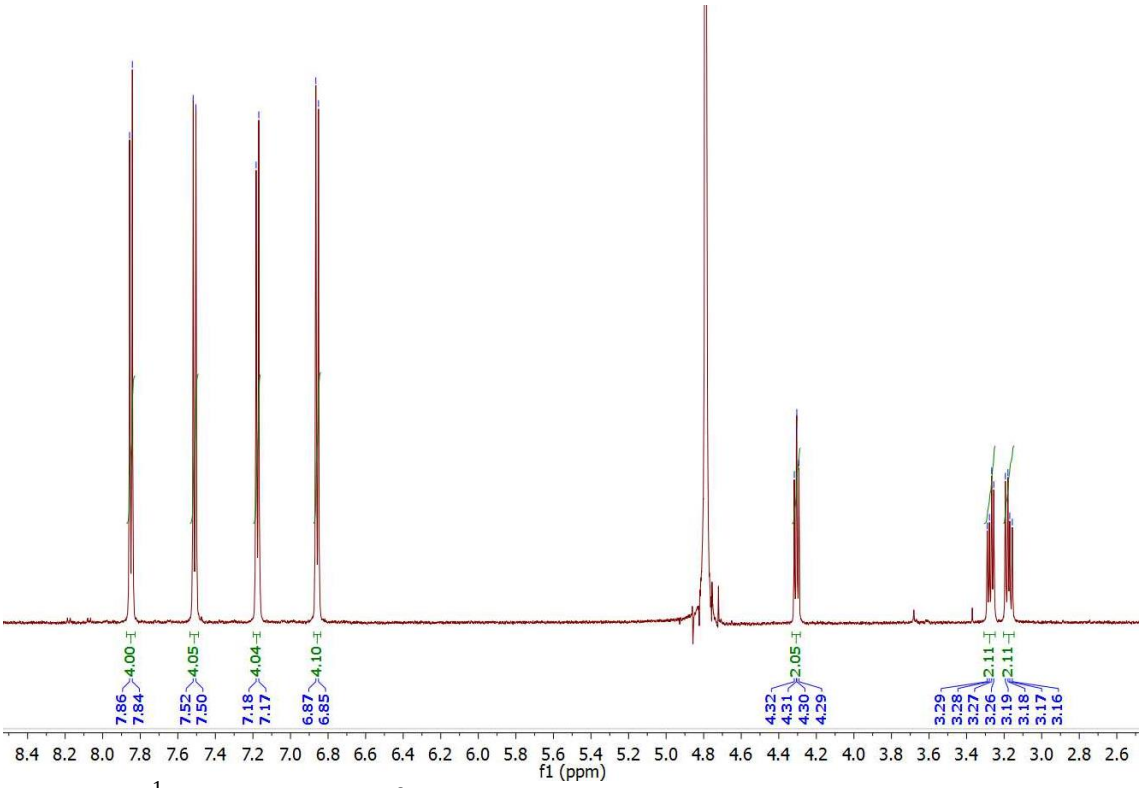

Figure S5. ^{1}H-NMR spectra of **4** (**Azo-LD-Tyr**).

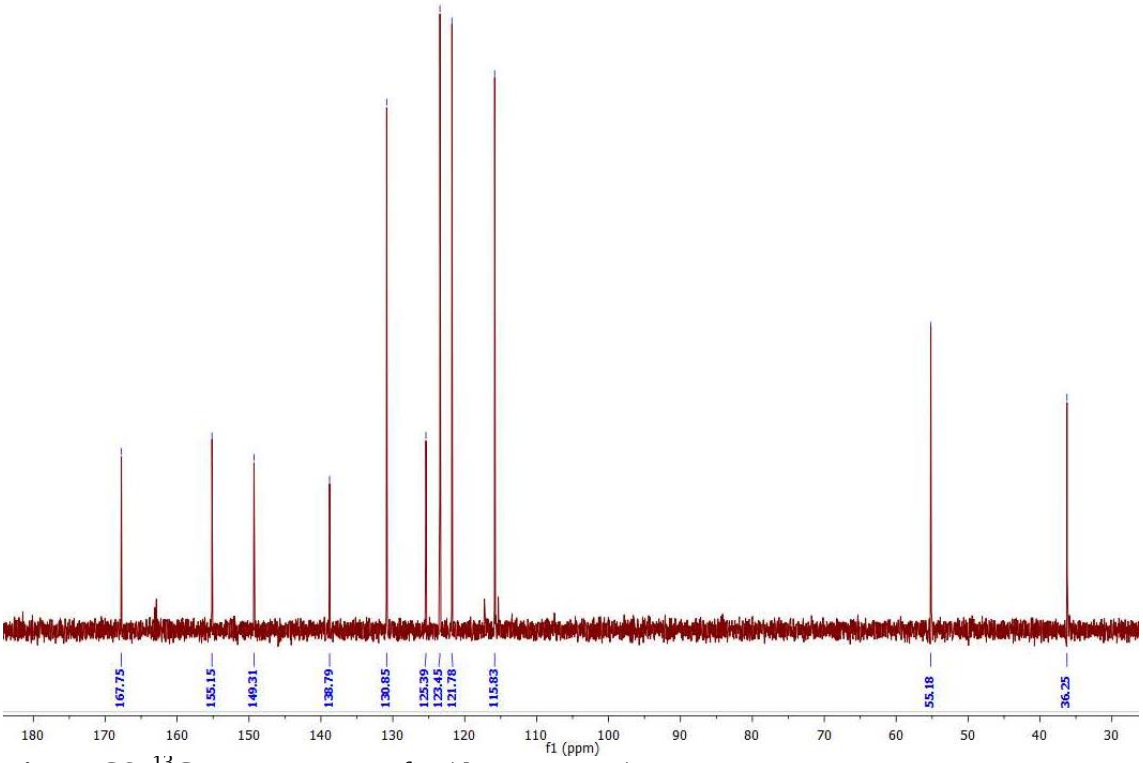

Figure S6. ^{13}C-NMR spectra of **4** (**Azo-LD-Tyr**).

Computations

Calculation of net charge of molecules 2-4 (Azo-DD-Tyr, Azo-LL-Tyr and Azo-LD-Tyr)

MarvinSketch package was used to predict the pKa values of polyamine side chains, and the numbers of charges distributed along the substituent chains were calculated at pH = 6.8.[1]

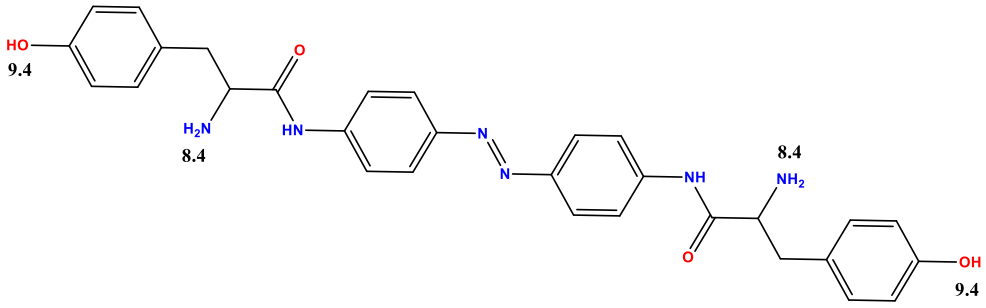

Figure S7. Calculated pKa values for molecules **2-4**.

The number of charges along the substituents can be estimated by using the following equations:

$Q_{molecule} = \sum Q^{-} + \sum Q^{+}$

For negatively charged fraction (-Ph-OH, pKa = 9.4)

$Q^{-} = \frac{(-1)}{1+10^{-(pH-pKa)}}$

$Q^{-} = \frac{(-1)}{1+10^{-(6.8-9.4)}}$

$Q^{-} = -2.5\ 10^{-3}$.

For positively charged fraction ($-NH_3^+$, pKa = 8.4)

$Q^{+} = \frac{(+1)}{1+10^{+(pH-pKa)}}$

$Q^{+} = \frac{(+1)}{1+10^{+(6.8-8.4)}}$

$Q^{+} = 0.98$

Based on these calculations the total charge for the molecules **2-4** is equal to:

$Q_{molecule(\mathbf{2\text{-}4})} = 1.96$

Electrostatic potential surface calculations

Calculations were carried out by Gaussian 09 package,[2] B3LYP functional with 6-31G(d,p) basis set was used.[3] Default PCM model was used in order to include solvent effects, with water as a solvent, all structures were confirmed as stationary points by frequency analysis. All optimized geometries were confirmed as a minimum by frequency analysis. Electrostatic potential surfaces (ESP) were calculated at 0.02 isovalue and 0.000400 density. We used fully protonated amino group and hydroxyl group in phenol side chain, which corresponds to the state of the molecules at pH = 6.8. Isovalue for ESP was set to 0.02.

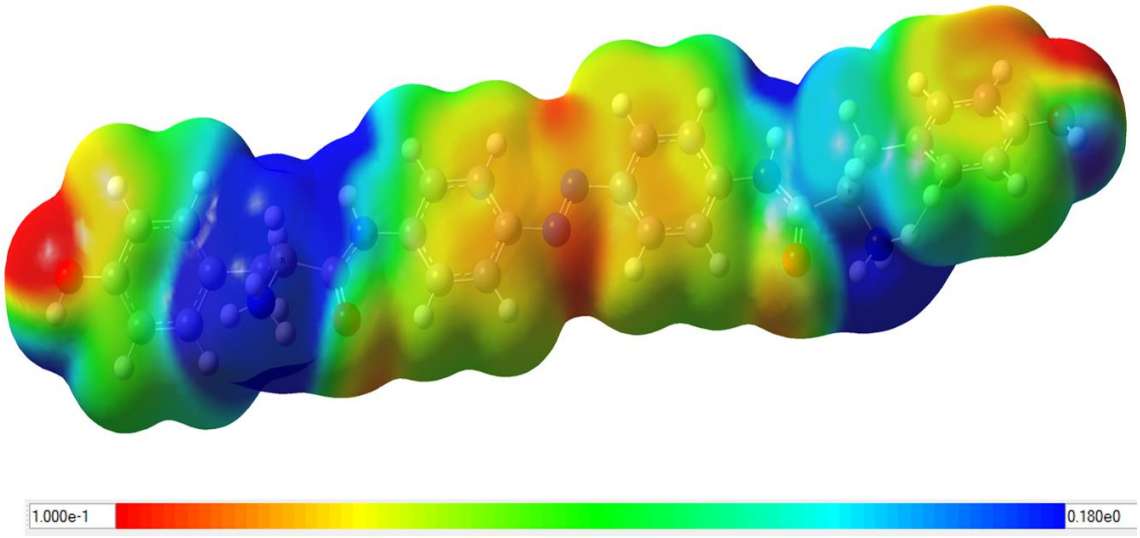

Figure S8. Electrostatic potential surface for **Azo-LL-Tyr** (*trans*).

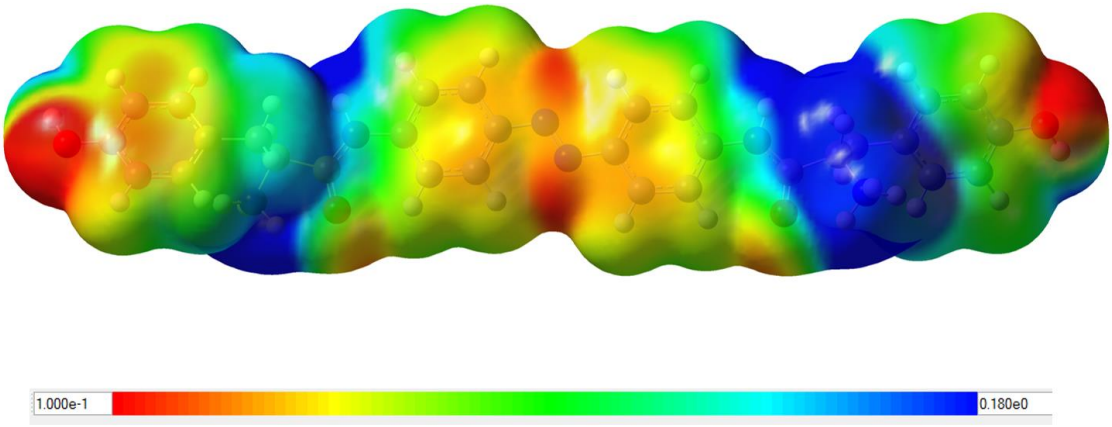

Figure S9. Electrostatic potential surface for **Azo-DD-Tyr** (*trans*).

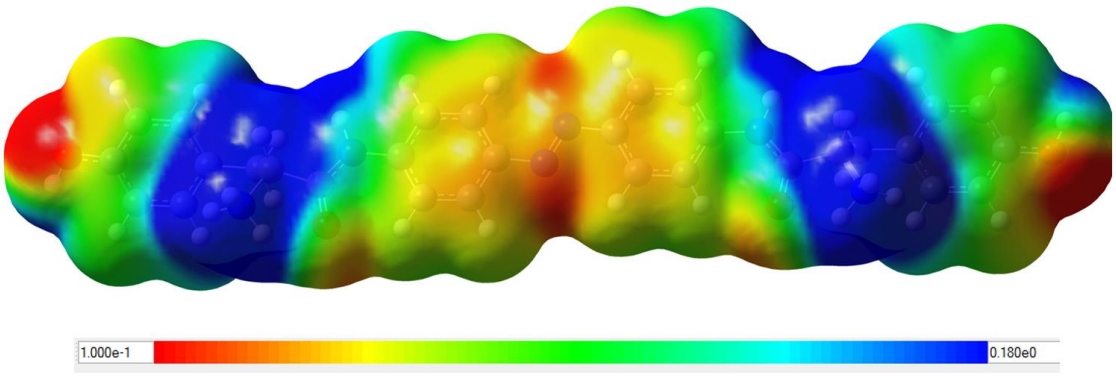

Figure S10. Electrostatic potential surface for **Azo-LD-Tyr** (*trans*).

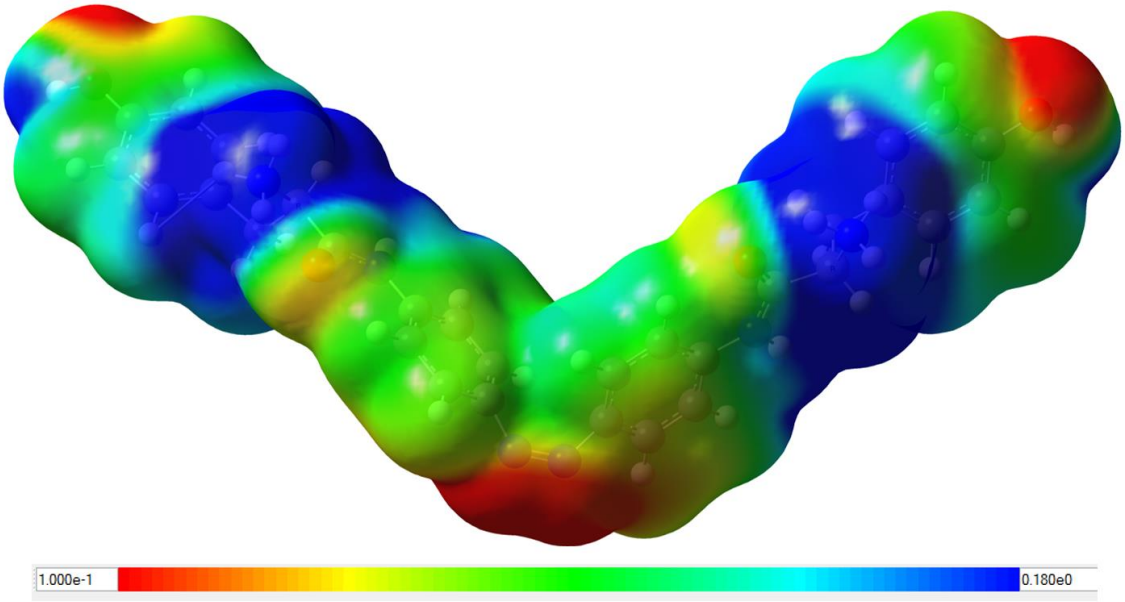

Figure S11. Electrostatic potential surface for **Azo-LL-Tyr** (*cis*).

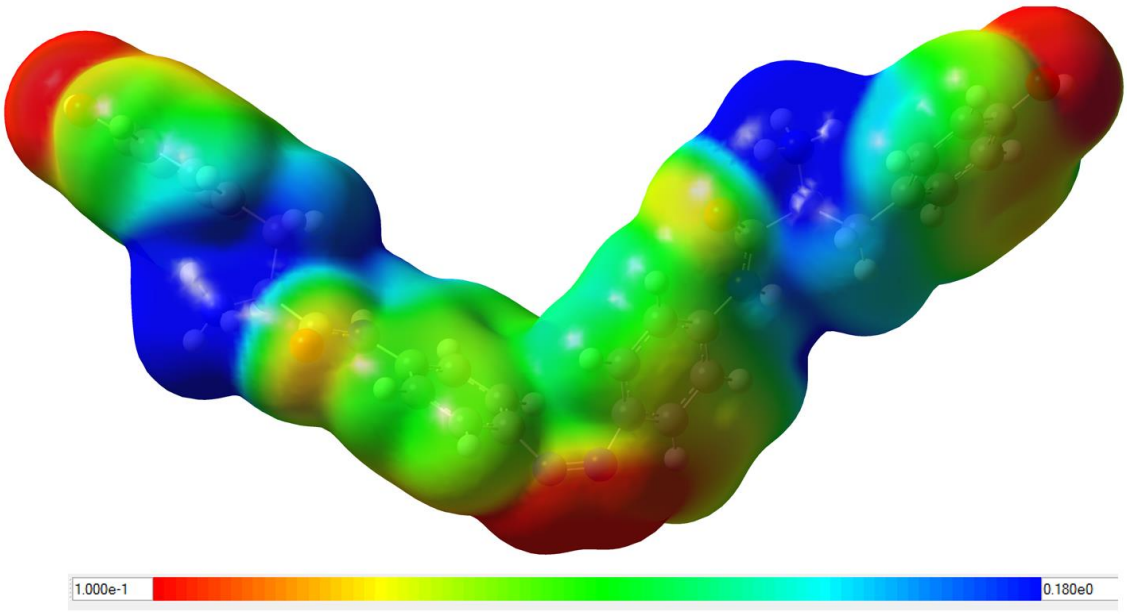

Figure S12. Electrostatic potential surface for **Azo-DD-Tyr** (*cis*).

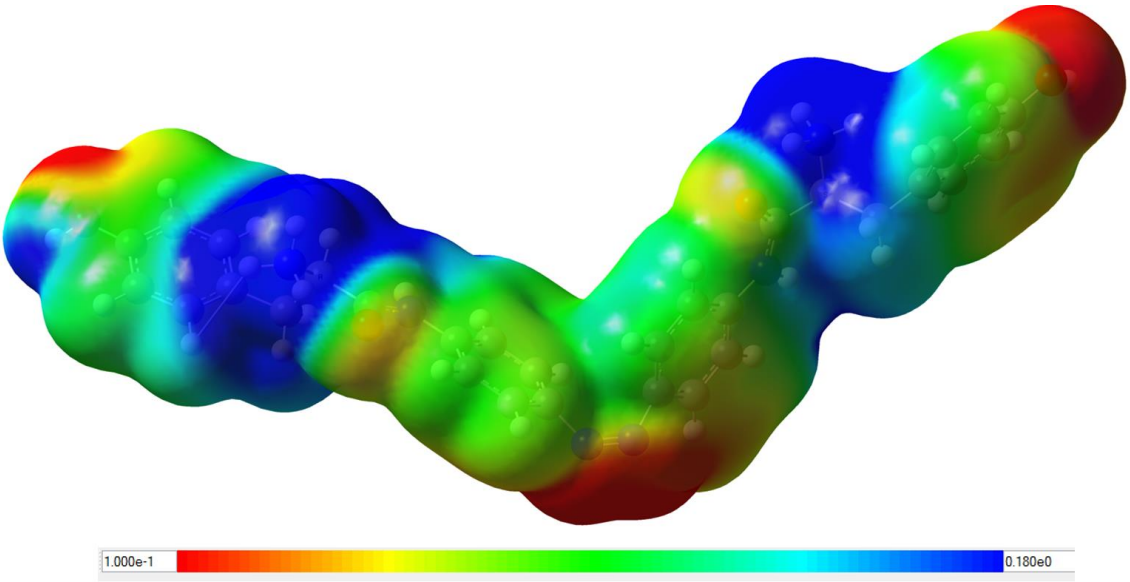

Figure S13. Electrostatic potential surface for **Azo-LD-Tyr** (*cis*).

Cartesian coordinates for **Azo-LL-Tyr** (*trans*)

C	-3.85913585	-1.26943160	0.29977162
C	-2.47612761	-1.29333042	0.13981835
C	-1.71679708	-0.11814875	0.19340550
C	-2.36185580	1.11163161	0.41467757
C	-3.73651977	1.14682554	0.57614692
C	-4.48992512	-0.03910623	0.51939111
H	-4.43441959	-2.18313060	0.25605454
H	-1.96121975	-2.23310356	-0.03121774

H	-1.77168701	2.01961722	0.45616912
H	-4.23298047	2.10008641	0.74771966
N	-0.32179616	-0.27944075	0.01473594
N	0.34081656	0.79299283	0.05398778
C	1.73633845	0.63317568	-0.12289027
C	2.39030999	-0.59565544	-0.31436067
C	2.48753418	1.81572126	-0.09728838
C	3.76796145	-0.64858709	-0.47879158
H	1.80171391	-1.50570066	-0.33195301
C	3.86578376	1.77481873	-0.26150169
H	1.97204077	2.75859567	0.05215243
C	4.50907137	0.54503984	-0.45255802
H	4.26619383	-1.59645111	-0.62662589
H	4.43929515	2.69897977	-0.24059818
N	5.92403532	0.58509007	-0.61283248
N	-5.89697192	0.09545031	0.69508700
H	-6.21095835	1.04840707	0.83860213
H	6.32261660	1.51565021	-0.56219450
C	6.78492161	-0.43008183	-0.82344085
C	8.28347892	-0.03933061	-0.86792551
O	6.50209294	-1.62475349	-0.94104797
C	8.88715380	0.15388781	0.55222997
H	8.47636795	1.08760475	0.95271989
H	8.51888988	-0.65281755	1.19718051
C	10.40016474	0.17525959	0.54181872
C	11.13478045	-0.94302950	0.96737092
C	11.11003364	1.29884668	0.07836511
H	10.61771946	-1.81044237	1.37463486
C	12.53085783	-0.94724945	0.93434153
C	12.49591827	1.30863927	0.04291102
H	10.57089489	2.18935965	-0.23885208
H	13.07925226	-1.81770125	1.28606460
C	13.21865337	0.18106956	0.47191223
H	13.04535840	2.17952361	-0.29888882
O	14.56575438	0.26289806	0.41045502
H	14.97665051	-0.54250820	0.76473457
C	-6.84657992	-0.86088904	0.69578659
C	-8.30536368	-0.35635116	0.82695244
O	-6.67042364	-2.07405882	0.56162984
C	-8.86574112	0.18805160	-0.51781185
H	-8.36590807	1.14384054	-0.71142148
H	-8.56100308	-0.49374701	-1.32068342
C	-10.37044382	0.34514093	-0.49728641
C	-11.19719797	-0.59067087	-1.13920297
C	-10.98244239	1.40966780	0.19067775
H	-10.75526522	-1.39902967	-1.71972607
C	-12.58836469	-0.47520949	-1.09915749
C	-12.36222846	1.53748419	0.23572370
H	-10.36973176	2.16390369	0.68068038
H	-13.20820026	-1.20165125	-1.61899838
C	-13.17793984	0.59164817	-0.41050186
H	-12.83533605	2.36620905	0.75200448
O	-14.51295144	0.78037008	-0.32505944
H	-14.98992064	0.10442745	-0.83361020
N	8.94373338	-1.22742141	-1.52487378
H	8.27580919	-2.01784626	-1.36289123

H	9.06463503	-1.11416541	-2.53588949
H	9.86851512	-1.40104959	-1.09502068
H	8.47649585	0.83616650	-1.49249075
H	-8.42992190	0.38084276	1.62378492
N	-9.07890615	-1.59226558	1.21852358
H	-8.47950475	-2.38784713	0.89469102
H	-9.20937099	-1.68283464	2.23065356
H	-10.00696800	-1.58869386	0.76149832

Cartesian coordinates for **Azo-DD-Tyr** (*trans*)

C	3.85708787	-1.26675753	0.30342274
C	2.47411062	-1.28961140	0.14329142
C	1.71620533	-0.11327069	0.19177336
C	2.36266135	1.11659163	0.40840323
C	3.73731996	1.15071855	0.57033562
C	4.48930246	-0.03634470	0.51844936
H	4.43126823	-2.18131297	0.26333943
H	1.95806535	-2.22942851	-0.02402339
H	1.77358889	2.02546211	0.44611036
H	4.23487939	2.10401972	0.73846055
N	0.32115674	-0.27388744	0.01353601
N	-0.34021458	0.79962069	0.04362174
C	-1.73592655	0.63928071	-0.13174719
C	-2.39102911	-0.59131715	-0.30718010
C	-2.48611473	1.82269487	-0.12153847
C	-3.76866770	-0.64520122	-0.47104259
H	-1.80331443	-1.50207442	-0.31263531
C	-3.86439421	1.78086621	-0.28570097
H	-1.96985295	2.76697946	0.01590297
C	-4.50881628	0.54928600	-0.46070328
H	-4.26764142	-1.59453631	-0.60612572
H	-4.43707470	2.70574541	-0.27691784
N	-5.92377555	0.58814834	-0.62189462
N	5.89641460	0.09701637	0.69451581
H	6.21139238	1.04983220	0.83678045
H	-6.32183019	1.51955451	-0.58552270
C	-6.78506311	-0.43007006	-0.81602367
C	-8.28415087	-0.04055651	-0.86642552
O	-6.50198773	-1.62633427	-0.91415214
N	-8.94299994	-1.24029582	-1.50364258
H	-8.47813577	0.82384578	-1.50598263
C	-8.88567591	0.17937361	0.55148988
H	-8.27538479	-2.02769722	-1.32648576
H	-8.51038410	-0.61144897	1.21188269
H	-8.47918645	1.12361484	0.93056679
C	-10.39863854	0.19048856	0.54717761
C	-11.12142751	1.31767899	0.12731352
C	-11.12104217	-0.95539160	0.93201273
H	-10.59654845	2.22721806	-0.15781247
C	-12.51199716	1.30767479	0.09077718
C	-12.51224206	-0.98071587	0.89406489
H	-10.59107835	-1.82702391	1.31377180
H	-13.05292585	2.19723517	-0.22329787
C	-13.21757194	0.15469426	0.47170472

H	-13.06868946	-1.85743077	1.20813165
O	-14.56596865	0.07062075	0.45970064
H	-14.96201691	0.91585467	0.19210987
C	6.84508055	-0.86028423	0.69628286
C	8.30434348	-0.35708990	0.82757102
O	6.66774637	-2.07336330	0.56299195
N	9.07678293	-1.59366369	1.21921270
H	8.42945120	0.37996799	1.62444120
C	8.86533439	0.18691606	-0.51705589
H	9.20695413	-1.68438689	2.23136504
H	8.56006813	-0.49447643	-1.32007668
H	8.36640714	1.14319344	-0.71060798
C	10.37018119	0.34264512	-0.49634427
C	11.19616094	-0.59361110	-1.13855901
C	10.98304607	1.40633284	0.19218910
H	10.75360683	-1.40132942	-1.71949784
C	12.58744492	-0.47941877	-1.09828103
C	12.36292444	1.53286985	0.23748758
H	10.37091706	2.16087706	0.68244332
H	13.20666443	-1.20619723	-1.61838257
C	13.17787989	0.58657221	-0.40905580
H	12.83674477	2.36090386	0.75422489
O	14.51304584	0.77405850	-0.32328849
H	14.98950217	0.09785944	-0.83198060
H	8.47674742	-2.38876482	0.89534568
H	-9.86943859	-1.40889252	-1.07490716
H	-9.05987593	-1.14498741	-2.51696181
H	10.00493146	-1.59085949	0.76234859

Cartesian coordinates for **Azo-LD-Tyr** (*trans*)

C	-3.88284251	1.39903732	-0.12790729
C	-2.49115925	1.44021524	-0.11042181
C	-1.72525520	0.37857368	-0.60732484
C	-2.37278416	-0.75292635	-1.13447928
C	-3.75613111	-0.80454593	-1.15656053
C	-4.51596529	0.26728946	-0.65545372
H	-4.46313046	2.22527902	0.25737241
H	-1.97428294	2.30497374	0.29280264
H	-1.77764102	-1.57324180	-1.51828202
H	-4.25448691	-1.68161439	-1.56523006
N	-0.32156366	0.54536294	-0.53127005
N	0.34806974	-0.42087721	-0.98814148
C	1.75213451	-0.25670744	-0.91185364
C	2.40618527	0.86566448	-0.37616158
C	2.51225238	-1.31858935	-1.41983746
C	3.79267193	0.93189022	-0.34558950
H	1.81063141	1.68252377	0.01494933
C	3.89945668	-1.26310443	-1.39466591
H	1.99643705	-2.18007734	-1.83074880
C	4.54278867	-0.14000850	-0.85847441
H	4.29105044	1.79792990	0.06691985
H	4.48004129	-2.09303204	-1.79169928
N	5.96713384	-0.15814245	-0.86656560
N	-5.93155276	0.12370786	-0.71855355

H	-6.24515987	-0.75683689	-1.11051465
H	6.37043618	-1.00002378	-1.26138817
C	6.83255550	0.77765390	-0.42851539
C	8.33107006	0.39144909	-0.50557726
O	6.54893962	1.87433876	0.05881153
C	8.76030287	-0.54040316	0.66413736
H	8.30581878	-0.16503416	1.58882069
H	8.31455348	-1.52264242	0.47188511
C	10.26278763	-0.63471683	0.81239267
C	11.03067086	-1.45439662	-0.02863879
C	10.93413501	0.13538052	1.78163965
H	10.54357082	-2.07868774	-0.77499199
C	12.41589725	-1.50777820	0.08809457
C	12.32019607	0.09684138	1.90399689
H	10.36256374	0.73809205	2.48639301
H	12.99055950	-2.16166760	-0.56363386
C	13.07105938	-0.72789124	1.05483617
H	12.83525990	0.67624734	2.66288763
O	14.41143788	-0.72595053	1.22460819
H	14.83663492	-1.35565357	0.61998350
C	-6.88978306	0.99133098	-0.33688680
C	-8.34586257	0.47865079	-0.46156491
O	-6.71869264	2.11804229	0.13405055
C	-8.74962153	-0.44420855	0.72339984
H	-8.21182631	-1.38989921	0.59245663
H	-8.37568721	0.00336483	1.65202990
C	-10.24445217	-0.66389677	0.80421854
C	-11.01851005	0.02454418	1.75217981
C	-10.90280153	-1.53389421	-0.08491913
H	-10.53479299	0.66779575	2.48569259
C	-12.40343692	-0.14342814	1.81573663
C	-12.27664081	-1.71234802	-0.03006787
H	-10.32924605	-2.09825679	-0.81759143
H	-12.98022795	0.38590242	2.57021704
C	-13.03942908	-1.01475625	0.92345929
H	-12.78409820	-2.39489408	-0.70368939
O	-14.37166100	-1.23907641	0.91829060
H	-14.80703725	-0.74747545	1.63371204
H	-8.54568715	-0.01057626	-1.41788145
N	-9.17609569	1.73826465	-0.40681468
H	-8.56351736	2.43297497	0.08151386
H	-9.40515821	2.11142458	-1.33311091
H	-10.05513282	1.56017928	0.10882147
H	8.60965214	-0.04475091	-1.46782936
N	9.04875972	1.71331653	-0.37562519
H	9.91648081	1.59566838	0.17541740
H	9.28573709	2.13368465	-1.27939917
H	8.35730291	2.33853726	0.10167447

Cartesian coordinates for **Azo-LL-Tyr** (*cis*)

N	-0.50512262	4.87373793	-0.78124404
N	0.69871801	4.79452829	-0.47358054
C	1.42095857	3.58900912	-0.21081954
C	1.37491630	2.45579959	-1.03779002

C	2.40950140	3.67538619	0.78033363
C	2.30776442	1.43901583	-0.86812946
H	0.64466707	2.38895893	-1.83685471
C	3.31927792	2.64498894	0.98350534
H	2.46743453	4.57721350	1.38161998
C	3.28157680	1.52794549	0.13665379
H	2.28722535	0.58018551	-1.53619286
H	4.07076786	2.72350409	1.75599422
C	-1.46901646	3.82188720	-0.68495550
C	-2.45110440	3.80624429	-1.68775165
C	-1.63471711	3.01490684	0.45054676
C	-3.55427786	2.97513712	-1.57300557
H	-2.34423954	4.46887795	-2.54051727
C	-2.76131277	2.20650164	0.59209325
H	-0.90394920	3.04884888	1.25152216
C	-3.72664594	2.18964669	-0.42357786
H	-4.30564167	2.97110201	-2.35985831
H	-2.89728605	1.61295847	1.48556620
C	-5.40386768	0.68232258	0.66547314
C	-6.78635859	0.02573763	0.42563307
O	-4.83061070	0.43890642	1.73062309
C	-6.69121438	-1.26794706	-0.43245206
H	-6.46005965	-0.95667105	-1.45723250
H	-5.83307012	-1.85290973	-0.08012931
C	-7.95603685	-2.09632623	-0.37733472
C	-9.08589214	-1.75724159	-1.13734375
C	-8.04174573	-3.21279139	0.47666862
H	-9.04902378	-0.91278961	-1.82255195
C	-10.25923013	-2.49968030	-1.05269636
C	-9.21174102	-3.96030453	0.57569384
H	-7.16542789	-3.53453049	1.03813266
H	-11.11809756	-2.22820659	-1.66186920
C	-10.33089893	-3.60635092	-0.19094480
H	-9.27180306	-4.83101287	1.22004033
O	-11.43496154	-4.37217643	-0.05421995
H	-12.14026887	-4.07202464	-0.65045313
N	-4.93665901	1.44009479	-0.34511905
N	4.23082584	0.46634871	0.21057457
H	-5.54909414	1.55787643	-1.14412131
H	4.10343748	-0.26029905	-0.48429395
C	5.30103431	0.34795571	1.02197255
C	6.24386973	-0.84450245	0.72478254
O	5.62024874	1.11481767	1.93361706
C	7.18680644	-0.56324997	-0.48056980
H	6.57077543	-0.59756358	-1.38631570
H	7.56057327	0.46401087	-0.39462761
C	8.33802149	-1.54189532	-0.55722064
C	9.62704620	-1.16456395	-0.14768964
C	8.14505780	-2.85991935	-1.01194841
H	9.82083858	-0.13930460	0.16364272
C	10.69195133	-2.06702726	-0.18644687
C	9.19443697	-3.76475221	-1.05838798
H	7.16295912	-3.17732291	-1.35734802
H	11.68535001	-1.74711538	0.11830542
C	10.48004325	-3.37318719	-0.64372303
H	9.05184053	-4.77615485	-1.42427333

O	11.45305771	-4.30704841	-0.71795291
H	12.31031337	-3.93436635	-0.45454080
N	7.07515501	-0.96719092	1.97887770
H	7.01196225	-0.02175652	2.42570226
H	6.70976585	-1.65798716	2.64115919
H	8.04768389	-1.22181096	1.73402711
H	5.70940542	-1.78716797	0.58491385
H	-7.51611963	0.71756651	-0.00181835
N	-7.25742165	-0.33457665	1.81394468
H	-6.37905298	-0.41210709	2.37715011
H	-7.84369638	0.38982478	2.24017441
H	-7.78772996	-1.22288642	1.79092285

Cartesian coordinates for **Azo-DD-Tyr** (*cis*)

N	0.76098363	4.82215418	0.03472944
N	-0.44372425	4.87783025	-0.27398701
C	-1.38324134	3.80428957	-0.17869780
C	-1.53189667	3.00437077	0.96494018
C	-2.35852445	3.75100990	-1.18508599
C	-2.64346602	2.17883864	1.09021784
H	-0.80894630	3.06087832	1.77141283
C	-3.44976950	2.89633899	-1.08711994
H	-2.25935035	4.40816274	-2.04330387
C	-3.60590473	2.12298907	0.07233806
H	-2.76993712	1.58946561	1.99630805
H	-4.18943012	2.86219547	-1.87409688
C	1.50693779	3.62929429	0.29049160
C	2.48459370	3.72368219	1.29326233
C	1.49815629	2.51149608	-0.55694939
C	3.40941918	2.70558308	1.46526840
H	2.51935280	4.61274034	1.91466278
C	2.45050424	1.50353933	-0.41698031
H	0.77352432	2.44688667	-1.36165983
C	3.41239937	1.60379302	0.59694474
H	4.16012322	2.79028988	2.24826628
H	2.45728254	0.66256792	-1.09663120
C	4.76341365	-0.43028868	0.04270936
C	6.10564535	-1.12051280	0.39120700
O	4.10954493	-0.88584405	-0.89939476
N	6.00474771	-2.46895970	-0.27948547
H	6.23173480	-1.29021819	1.46324425
C	7.32886158	-0.35228366	-0.18928211
H	5.28762930	-2.33358988	-1.03026081
H	7.08597478	-0.03860386	-1.21165140
H	7.44286573	0.56386565	0.40047554
C	8.59530683	-1.17939455	-0.17549194
C	9.34885735	-1.34334456	0.99681836
C	9.02928329	-1.83932436	-1.34152294
H	9.05467078	-0.83094702	1.91056969
C	10.49305154	-2.13435615	1.01111936
C	10.16825398	-2.63960144	-1.33884892
H	8.49958348	-1.68478828	-2.28077018
H	11.07198204	-2.23489025	1.92616817
C	10.90879520	-2.79181197	-0.15830826

H	10.51366554	-3.13157144	-2.24192733
O	12.00604280	-3.57717920	-0.21918464
H	12.47510700	-3.58192820	0.63105294
H	6.92611071	-2.74531492	-0.66223134
H	5.67444315	-3.20805434	0.34807897
N	4.46054423	0.65504967	0.78077889
N	-4.74327065	1.29486346	0.30531333
H	5.10063757	0.88536250	1.53218402
H	-4.74466865	0.82628781	1.20382556
C	-5.83457611	1.12571386	-0.46776630
C	-6.91640041	0.16574907	0.08967800
O	-6.03520747	1.62869256	-1.57576015
N	-8.14488232	0.50636477	-0.71949962
H	-7.14934328	0.35453254	1.14036921
C	-6.55687881	-1.33153119	-0.13062999
H	-7.76883733	0.94549182	-1.59281513
H	-8.69309180	-0.34865242	-0.91542103
H	-8.75330916	1.19009200	-0.25870043
H	-6.14986917	-1.44331873	-1.14268860
H	-5.74385396	-1.57143996	0.56381976
C	-7.74316059	-2.24990353	0.06618677
C	-8.19410935	-2.59889661	1.34837546
C	-8.45500273	-2.74272158	-1.04445048
H	-7.65762602	-2.25095358	2.22889242
C	-9.31195211	-3.40864386	1.52218614
C	-9.57862405	-3.54845086	-0.88444068
H	-8.10025485	-2.53212778	-2.05250226
H	-9.63623653	-3.67848183	2.52445675
C	-10.01503997	-3.88647164	0.40425290
H	-10.11679234	-3.94161676	-1.74042472
O	-11.10906927	-4.67345248	0.49458220
H	-11.31401205	-4.87607741	1.42188102

Cartesian coordinates for **Azo-LD-Tyr** (*cis*)

N	-0.62424909	-4.38346501	0.36582105
N	0.55967307	-4.36352012	-0.01942478
C	1.38593649	-3.20225951	-0.13385820
C	1.51068869	-2.23118367	0.87186761
C	2.29518996	-3.20451720	-1.20175591
C	2.53120513	-1.28989477	0.79974953
H	0.84371308	-2.23814066	1.72704400
C	3.29246859	-2.24207474	-1.30250604
H	2.22069266	-3.98900284	-1.94824873
C	3.42508921	-1.29124668	-0.28042873
H	2.64272154	-0.56268849	1.60167792
H	3.98054602	-2.25298959	-2.13566145
C	-1.47594327	-3.24592235	0.52422283
C	-2.38837224	-3.31544901	1.58872313
C	-1.62333818	-2.23873524	-0.44113464
C	-3.40101362	-2.37597608	1.70435793
H	-2.30167815	-4.12601943	2.30509470
C	-2.66266039	-1.31444346	-0.35361842
H	-0.95132422	-2.19968977	-1.29182214
C	-3.55683520	-1.38589958	0.72297112

H	-4.09870572	-2.43959293	2.53682885
H	-2.78743189	-0.56077588	-1.11888323
C	-5.10457381	0.46536614	0.05462185
C	-6.49130804	1.06427833	0.39685673
O	-4.52380752	0.89454426	-0.94611742
N	-6.52211367	2.36492405	-0.36863201
H	-6.60577268	1.29918886	1.45782914
C	-7.65800502	0.15750822	-0.09329930
H	-5.82091058	2.23208420	-1.13458984
H	-7.41222838	-0.20719350	-1.09785023
H	-7.68009404	-0.72033897	0.56178613
C	-8.98987419	0.87470143	-0.10100623
C	-9.73134418	1.05326440	1.07689273
C	-9.50260647	1.41475938	-1.29647139
H	-9.37592175	0.63069750	2.01446079
C	-10.93917945	1.74329493	1.06831134
C	-10.70618212	2.11383395	-1.31734188
H	-8.98061100	1.24238898	-2.23697503
H	-11.50633617	1.85600120	1.98929109
C	-11.43348498	2.28217982	-0.13076295
H	-11.11071390	2.51227000	-2.24172263
O	-12.59555324	2.96551428	-0.21487248
H	-13.04621143	2.98773948	0.64499494
H	-7.47471400	2.53856769	-0.73490181
H	-6.23292878	3.17108282	0.19324692
N	-4.68318156	-0.52396623	0.86564210
N	4.47446483	-0.32611227	-0.24931363
H	-5.27258249	-0.74081688	1.66124539
H	4.47206530	0.27002749	0.57027495
C	5.49776706	-0.16549166	-1.11224522
C	6.58281840	0.85575864	-0.68812267
O	5.67309169	-0.78104364	-2.16652083
C	7.54999301	0.27609266	0.38397545
H	6.99141388	0.21912490	1.32514246
H	7.79896487	-0.75457801	0.10463058
C	8.80851642	1.10196646	0.53703185
C	10.02364254	0.66328180	-0.01302587
C	8.79098150	2.34048169	1.20577318
H	10.08180060	-0.31114680	-0.49536290
C	11.18615150	1.42923500	0.09608610
C	9.93852946	3.10943530	1.32323654
H	7.87031336	2.69891964	1.66237119
H	12.11986025	1.06061697	-0.32143628
C	11.14856229	2.65765309	0.76662963
H	9.93167904	4.05647064	1.85261329
O	12.22474662	3.45891396	0.92188381
H	13.01977538	3.04669646	0.54611085
N	7.35500162	1.10982028	-1.96010676
H	7.15528033	0.27182469	-2.55653338
H	7.04045358	1.94353205	-2.46530336
H	8.36256251	1.20986236	-1.74726185
H	6.16442038	1.80869835	-0.35535748

Experimental

Materials

Common reagent-grade chemicals were used without further purification. Human serum albumin (HSA), Warfarin and Digitoxin were purchased from Sigma Aldrich Chem. Co. Deionized water was used throughout all experiments. HSA, **Azo-LL-Tyr**, **Azo-DD-Tyr** and **Azo-LD-Tyr** were dissolved in deionized water and kept under dark, except during photoirradiation. HSA concentration was determined by absorption spectroscopy.

Sample irradiation

The photo-induced isomerization reactions of **Azo-LL-Tyr**, **Azo-DD-Tyr** and **Azo-LD-Tyr** were performed by using a high pressure Hg Oriel lamp equipped with interference filters at 360 and 436 nm. The resulting light intensity was 0.41 mW/cm^2 at 360 nm (*trans*-*cis*) and 1.04 mW/cm^2 at 436 nm (*cis*-*trans*).

The **Azo-LL-Tyr**, **Azo-DD-Tyr** and **Azo-LD-Tyr** *trans*-to-*cis* and *cis*-to-*trans* ratio was assessed by ^{1}H NMR spectroscopy according to the intensity ratios of the corresponding signals (data not shown). The *trans*:*cis* and *cis*:*trans* composition of the photostationary state was found to be 80:20 in both direction for all the studied light-activated compounds. UV irradiation does not affect the protein secondary structure as reported by us previously.[4]

UV/Vis spectroscopy

The UV-Vis absorption spectra were recorded on a Hitachi U-2900 spectrophotometer at 298 K. The concentration of the azobenzene derivatives (20 μM) was kept constant while incremental additions of HSA were added into the solution. Quantitative data analysis based on the UV-Vis titration takes into account the composition of the photostationary state.

Fluorescent measurements

Steady-state fluorescence studies were carried out with a Hitachi F-7000 spectrofluorometer. The HSA concentration was kept constant (5 μM) and samples were titrated with incremental addition of **Azo-LL-Tyr**, **Azo-DD-Tyr** and **Azo-LD-Tyr** until no appreciable changes of the emission intensity were seen, indicating saturation of the interaction. Under those circumstances the quantitative binding data analysis was carried out taking into account not only the composition of the photostationary state but also the inner filter effect (IFE).

$$F_{corr} = F_{obs} \times 10^{(A_{ex}+A_{em})/2} \quad (1)$$

Time-resolved fluorescence

Fluorescence lifetimes were measured via Time-Correlated Single Photon Counting (TCSPC) setup purchased from Becker&Hickl GmBH, where a BDL – 375 picosecond Laser Diode, emitting at 375 nm and operating with 20 MHz repetition rate, was used as excitation source. The signals were detected by a hybrid GaAs photodetector HPM - 100 - 50. The operation of this setup was controlled by a DCC-100 detector control card. The PL decay curves were averaged 10 times to increase the S/N ratio.

Circular dichroism

CD measurements were performed at 298 K in the wavelength range of 180-300 nm at different photochrome/HSA ratios and keeping constant the HSA concentration. Conversely, the concentration of molecular photoswitches was kept constant and incremental additions of HSA were added. Before use, the optical chamber of the CD spectrometer was deoxygenated with dry nitrogen and was held under nitrogen atmosphere during the measurements. Each spectrum was averaged from five successive accumulations. The protein secondary structure was computed by using the neural network K2D3 software as described in previously reported protocols.[5]

Azo-DD-Tyr and Azo-LD-Tyr photoisomerization

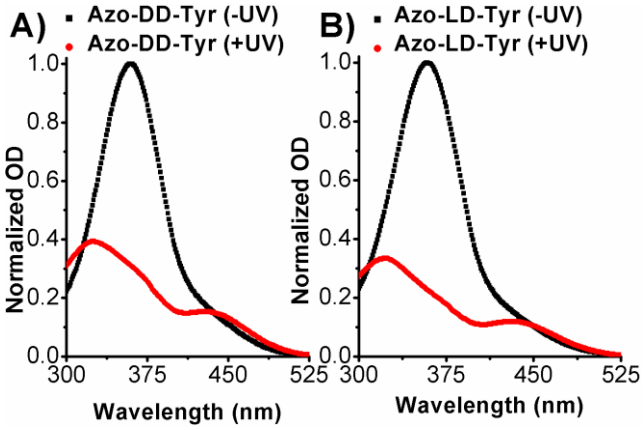

Figure S14. Photoisomerization process of **Azo-DD-Tyr** and **Azo-LD-Tyr** before (black like) and after (red line) UV irradiation.

UV-Vis spectral changes

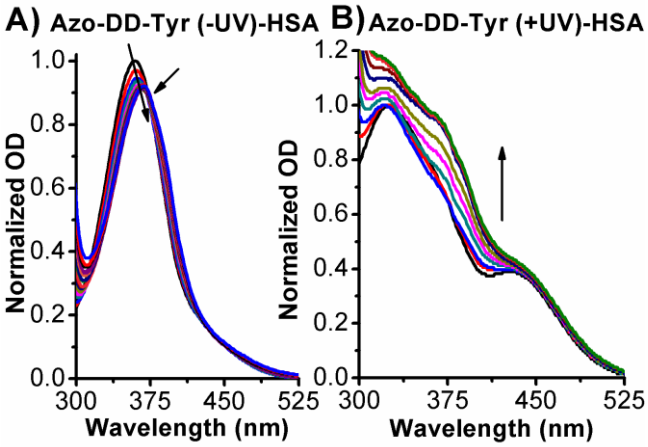

Figure S15. A) UV-Vis absorption change of **Azo-DD-Tyr** (no UV) upon addition of HSA (0-42.5 μM). **B)** UV-Vis absorption change of **Azo-DD-Tyr** (UV) upon addition of HSA (0-36 μM).

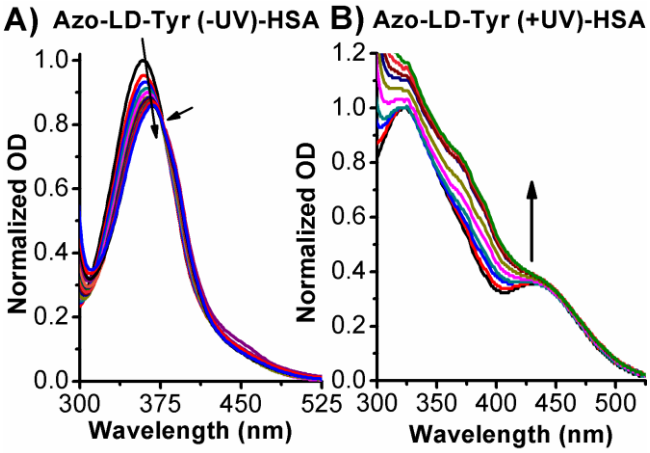

Figure S16. A) UV-Vis absorption change of **Azo-LD-Tyr** (no UV) upon addition of HSA (0-42.5 μM). **B)** UV-Vis absorption change of **Azo-LD-Tyr** (UV) upon addition of HSA (0-36 μM).

Scatchard plots

When small molecules bind to a set of equivalent sites on a macromolecule, the equilibrium association binding constant (Ka) can be examined according to the linear Scatchard analysis based on the following equation:[6]

$$\frac{r}{D_f} = nK_a - rK_a \qquad (2)$$

where r is the number of mole of ligand bound per mole of macromolecule and D_f is the molar concentration of the free ligand. The binding isotherms, obtained by Scatchard analysis were linear ($R^2 \approx 0.99$) indicating no deviations from Clark's model.

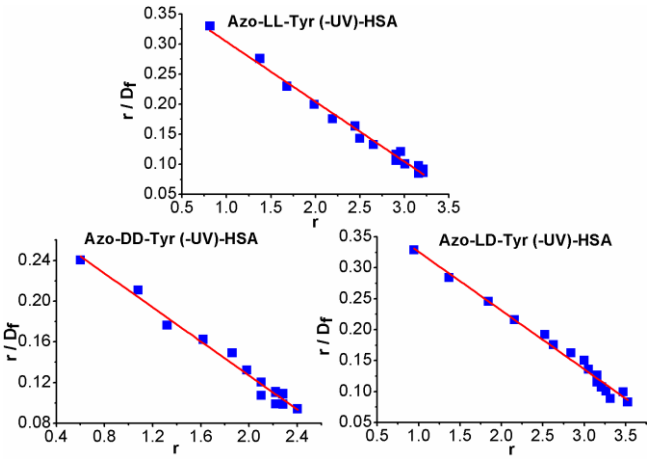

Figure S17. Scatchard plots for **Azo-LL-Tyr** (no UV)-HSA, **Azo-DD-Tyr** (no UV)-HSA and **Azo-LD-Tyr** (no UV)-HSA systems.

Benesi-Hildebrand plots

Exploiting the absorption changes arising upon HSA addition to **Azo-LL-Tyr** (UV), **Azo-DD-Tyr** (UV) and **Azo-LD-Tyr** (UV) it was possible to quantitatively calculate the binding affinity. Thus, the equilibrium association binding constants (K_a) was estimated by using the Benesi-Hildebrand equation:[7]

$$1/(A - A_0) = 1/(A_\infty - A_0) + 1/[HSA] \cdot 1/K_a(A_\infty - A_0) \quad (3)$$

where A_0 and A are the absorbances of the photochromes in the absence and in the presence of HSA, respectively, A_∞ is the final absorbance of the photochrome-HSA adduct. The plot of $1/(A\text{-}A_0)$ versus $1/C_{HSA}$ is linear and the binding constant can be calculated from the ratio of the intercept and the slope.

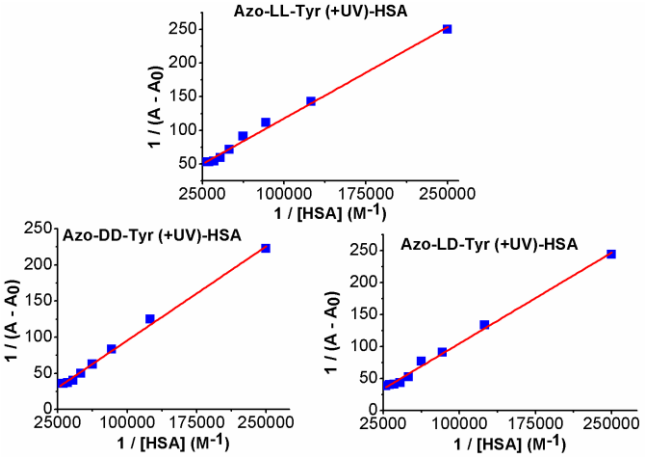

Figure S18. Plot of $1/(A\text{-}A_0)$ against 1/[HSA] for **Azo-LL-Tyr** (UV), **Azo-DD-Tyr** (UV) and **Azo-LD-Tyr** (UV)-HSA systems.

Mole ratio plots

The binding site size was calculated according to the mole ratio method. The inflection point of each graph is found to be close to 1 indicating a stoichiometry HSA:ABs equal to 1:1.These findings are in excellent agreement with the linearity of the aforesaid methods reported to calculate the binding affinity.

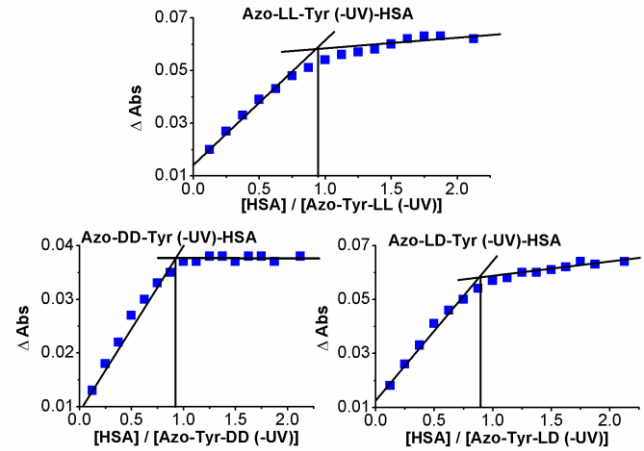

Figure S19. Plots of ΔAbs *vs*. the mole ratio for **Azo-Tyr-LL** (no UV), **Azo-Tyr-DD** (no UV) and **Azo-Tyr-LD** (no UV)-HSA systems.

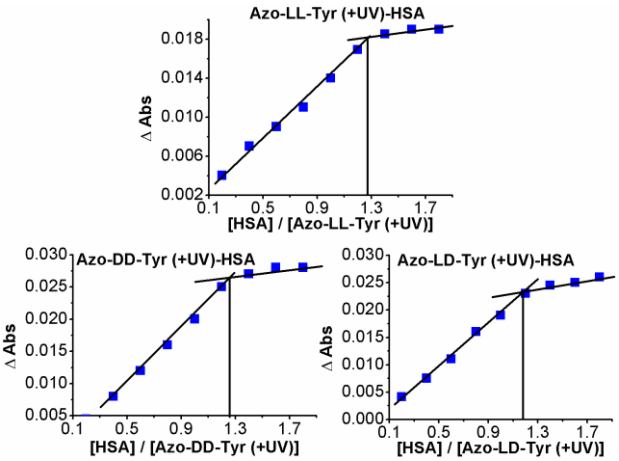

Figure S20. Plots of ΔAbs *vs*. the mole ratio for **Azo-LL-Tyr** (UV), **Azo-DD-Tyr** (UV) and **Azo-LD-Tyr** (UV)-HSA systems.

Hill Plots

The Hill slope analysis allowed to investigate whether the complexation process is involved in any cooperativity coordination since it takes into account the possibility that not all the receptor sites are independent (Data shown only for **Azo-LL-Tyr** (no UV), **Azo-DD-Tyr** (no UV) and **Azo-LD-Tyr** (no UV)-HSA systems). The Hill analysis is based on the following equation:[8]

$$log\left[\frac{B}{(B_{max}-B)}\right] = n\left[log\left(L_f\right)\right] - log(K_d) \qquad (4)$$

where B and B_{max} are the bound ligand and the total receptor concentration, respectively, L_f is the free ligand concentration and K_d is the equilibrium dissociation constant. Please note that B_{max} is extrapolated by the Scatchard analysis. The Hill coefficient was found to be: **Azo-LL-Tyr-HSA** (n_{Hill} = 1.01), **Azo-DD-Tyr-HSA** (n_{Hill} = 1.06) and **Azo-LD-Tyr-HSA** (n_{Hill} = 1.03). This value indicate that only a single class of binding sites is involved in the complexation process in agreement with the linearity of the fitting models and the mole ratio plots. Similar conclusions can be obtained also by plotting B *vs*. L_f which gives a hyperbolic shape (data not shown).

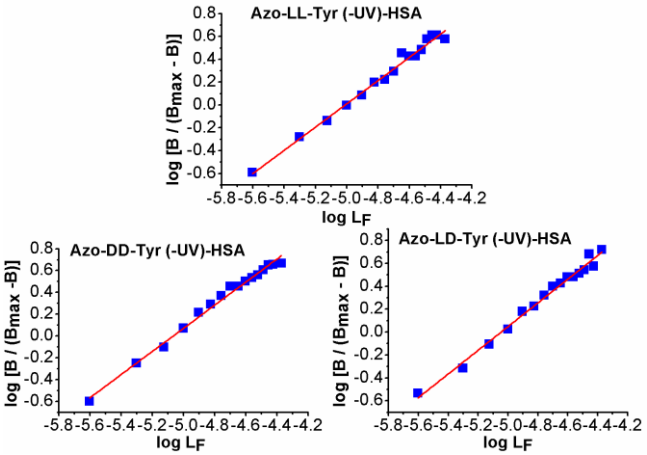

Figure S21. Hill plots for **Azo-LL-Tyr**, **Azo-DD-Tyr** and **Azo-LD-Tyr**-HSA systems.

Steady-state fluorescence properties for the free ABs

The fluorescence properties of the molecular photoswitches in their free state were investigated by steady state and time-resolved fluorescence measurements in the presence and absence of UV irradiation. The fluorescence maximum for **Azo-LL-Tyr** (UV/no UV) and **Azo-DD-Tyr** (UV/no UV) is centered at 400 nm, while **Azo-LD-Tyr** present a shoulder at 400 nm and maximum at 445 nm (Fig. S22). We speculate that the different spatial distribution of the substitution patterns in the **Azo-LD-Tyr** configuration may cause distortion of the symmetry and therefore partial changes in the transition dipole moment of the excited state level of the fluorophore resulting in a shift of the emission maximum toward longer wavelengths.

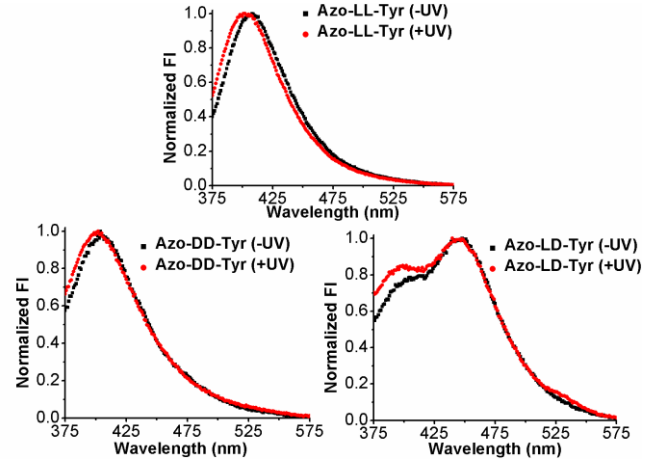

Figure S22. Fluorescence spectra of **Azo-LL-Tyr** (UV/no UV), **Azo-DD-Tyr** (UV/no UV) and **Azo-LD-Tyr** (UV/no UV) at 298 K. λ_{exc}: 320 nm.

Fluorescence quantum yields (φ_f) were calculated according to the comparative method of Williams using Hoechst 33258 (φ_f : 3.4 %) as standard reference (Table S1).[9]

Table S1. Calculated PLQY for each photochrome in the presence and absence of UV irradiation.

Sample	φ_f (%)
Azo-LL-Tyr (no UV)	0.1
Azo-LL-Tyr (UV)	0.05
Azo-DD-Tyr (no UV)	0.05
Azo-DD-Tyr (UV)	0.06
Azo-LD-Tyr (no UV)	0.07
Azo-LD-Tyr (UV)	0.05

Time-Correlated Single Photon Counting (TCSPC)

The PL decay traces for **Azo-LL-Tyr** (UV/no UV), **Azo-DD-Tyr** (UV/no UV) and **Azo-LD-Tyr** (UV/no UV) systems were fitted using double exponential function, with the sum of two amplitudes normalized to unity. Then the averaged fluorescence lifetimes were calculated according to Eq. 5:

$$\langle \tau \rangle = \frac{\sum A_i \tau_i^2}{\sum A_i \tau_i} \qquad (5)$$

where A_i is the *i-th* relative amplitude and τ_i is the *i-th* component of fluorescence lifetime, respectively.

The derived averaged lifetime values were used to estimate the radiative (k_r) and non-radiative (k_{nr}) decay rates by using the following equations:

$$\varphi_f = \frac{k_r}{k_r + k_{nr}} \tag{6}$$

$$< \tau > = \frac{1}{k_r + k_{nr}} \tag{7}$$

The fluorescence decay profile for each studied system and the relative photophysical parameters are shown in Figure S23-25 and Table S2. Each photochromic units studied can be properly described by using a double exponential function which can be the outcome of the presence in solution of at least two well-defined stable isomeric geometries (*trans* and *cis* configurations). It turns out that being the relative population of the excited state energy level not degenerate a different decay profile of the lifetime of the excited state can occur leading to a complex and at least bi-exponential deactivation pathway.

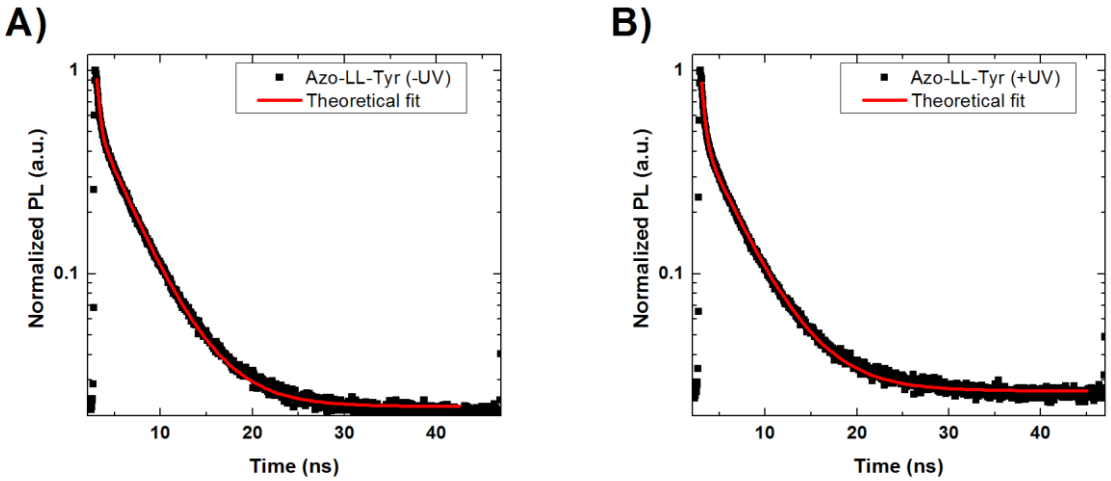

Figure S23. A) Fluorescence decay curves of **Azo-LL-Tyr** (no UV) and **B) Azo-LL-Tyr** (UV). The red line corresponds to bi-exponential fitting curve. λ_{exc} = 375 nm.

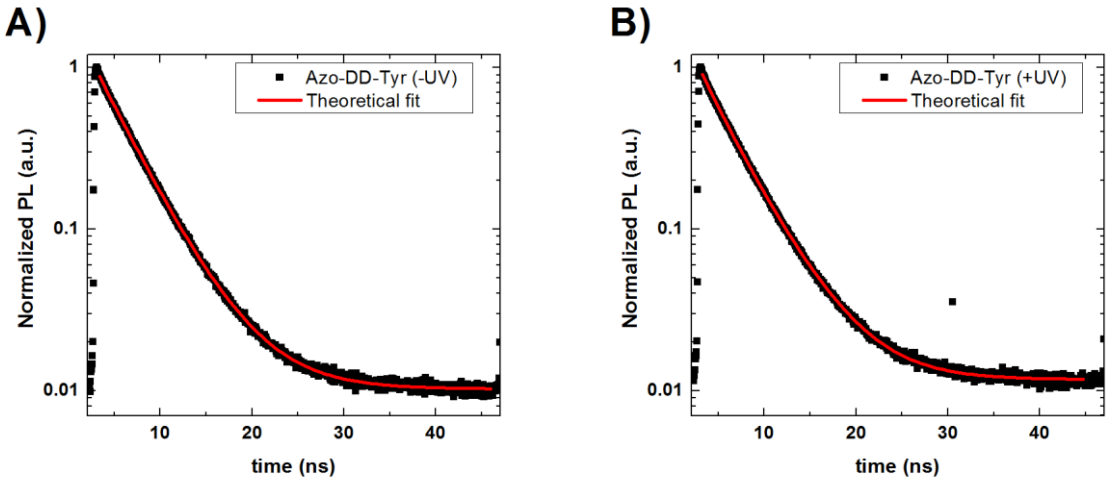

Figure S24. A) Fluorescence decay curves of **Azo-DD-Tyr** (no UV) and **B) Azo-DD-Tyr** (UV). The red line corresponds to biexponential fitting curve. λ_{exc} = 375 nm.

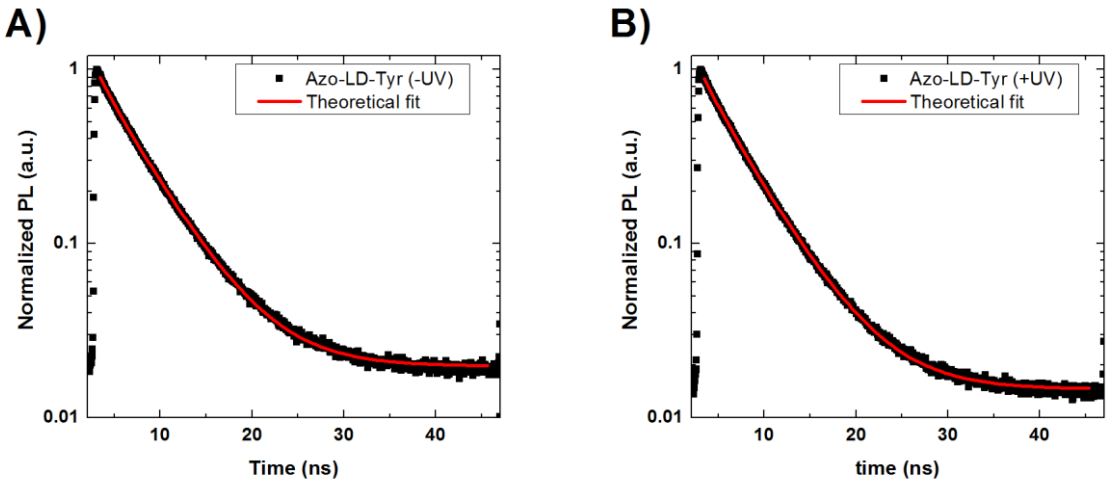

Figure S25. A) Fluorescence decay curves of **Azo-LD-Tyr** (no UV) and **B) Azo-LD-Tyr** (UV). The red line corresponds to biexponential fitting curve. λ_{exc} = 375 nm.

Table S2. Photophysical data for **Azo-LL-Tyr** (UV/no UV), **Azo-DD-Tyr** (UV/no UV) and **Azo-LD-Tyr** (UV/no UV).

Systems:	τ_1	τ_2	A_1	A_2	$\langle\tau\rangle$	k_r	k_{nr}
	ns	ns	%	%	ns	($\times10^5 s^{-1}$)	($\times10^8 s^{-1}$)
Azo-LL-Tyr (no UV)	0.46	4.10	25.1	74.9	3.97	2.32	2.52
Azo-LL-Tyr (UV)	0.50	4.18	29.0	71.0	4.00	1.09	2.49
Azo-DD-Tyr (no UV)	0.46	3.95	6.6	93.4	3.92	1.19	2.55
Azo-DD-Tyr (UV)	0.53	4.00	11.1	88.9	3.94	1.63	2.54
Azo-LD-Tyr (no UV)	1.01	4.86	20.4	79.6	4.65	1.39	2.15
Azo-LD-Tyr (UV)	1.27	4.77	16.3	83.7	4.59	1.01	2.18

τ_1 and τ_2: lifetime decay components, A_1 and A_2: relative amplitudes with their sum normalized to unity, $\langle\tau\rangle$: average lifetime, k_r: radiative decay rate, and k_{nr}: nonradiative decay rate.

Spectral overlap between HSA and the photochromes

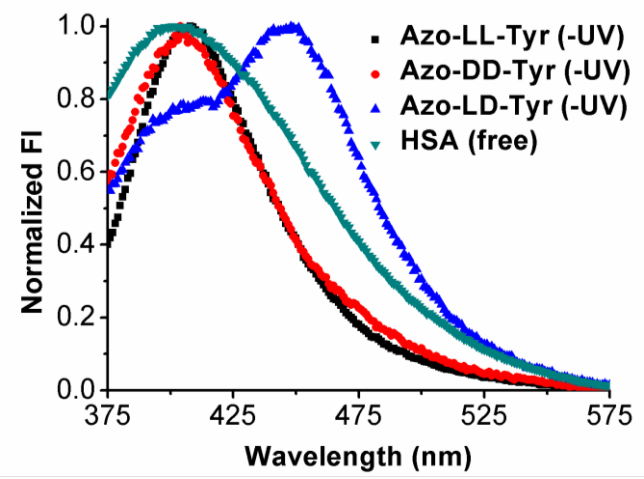

Figure S26. Emission spectra of **Azo-LL-Tyr** (no UV), **Azo-DD-Tyr** (no UV), **Azo-LD-Tyr** (no UV) and free HSA. λ_{exc}: 320 nm.

Fluorescence spectral changes on the HSA emission

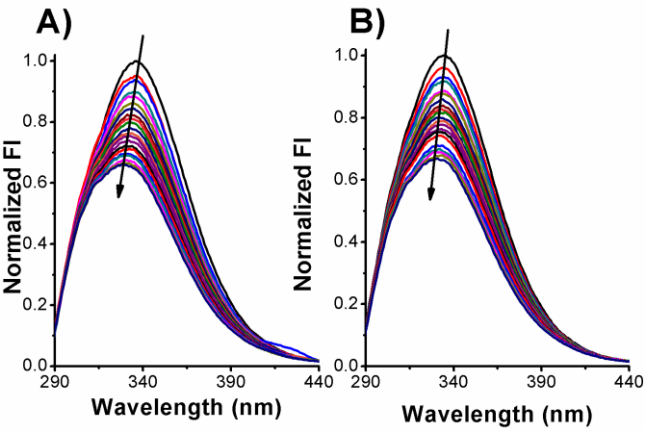

Figure S27. A) Fluorescent spectra changes of HSA upon addition of **Azo-DD-Tyr** (no UV) (0-10 μM). **B)** Fluorescent spectra changes of HSA upon addition of **Azo-LD-Tyr** (no UV) (0-10 μM).

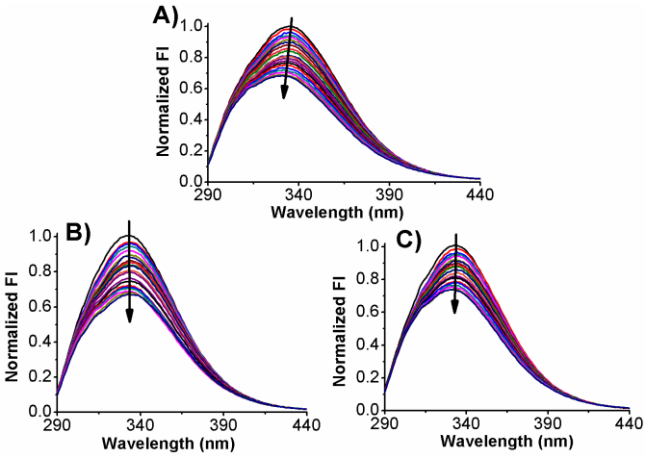

Figure S28. A) Fluorescent spectra changes of HSA upon addition of **Azo-LL-Tyr** (UV) (0-10 μM). **B)** Fluorescent spectra changes of HSA upon addition of **Azo-DD-Tyr** (UV) (0-10 μM). **C)** Fluorescent spectra changes of HSA upon addition of **Azo-LD-Tyr** (UV) (0-10 μM).

Stern-Volmer analysis

It is known that the quenching mechanisms encountered in the study of biological systems can be properly described by using the Stern-Volmer analysis.[10] The nature of quenching is usually classified as either dynamic or static.[10] Dynamic quenching results from the diffusive collisions of the excited fluorophore and the quencher, whereas static quenching is usually observed when the fluorophore and the quencher form a stable non-fluorescent ground-state complex.[10] In order to distinguish between these two different types of mechanism we processed our data using the following equation:[10]

$$\frac{F_0}{F} = 1 + k_q \tau_0 [Q] = 1 + K_{sv}[Q] \qquad (8)$$

where F_0 and F are the emission intensities of the protein in absence and presence of the photochrome, k_q is the bimolecular quenching rate constant, τ_0 is the average excited-state lifetime of HSA taken as 3.53 ns,[11] K_{sv} is the Stern-Volmer constant and [Q] is the concentration of the ABs.

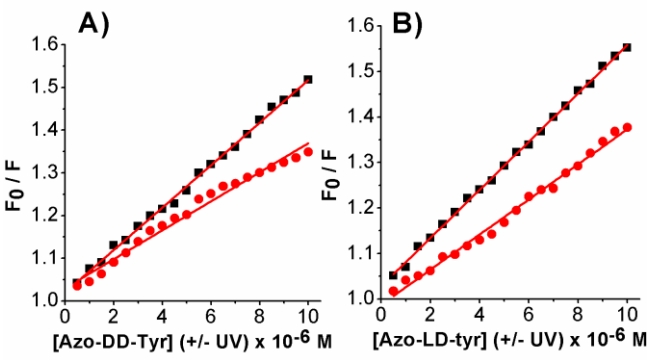

Figure S29. A) Stern-Volmer plot of the fluorescence quenching of the **Azo-DD-Tyr** (no UV)-HSA (black squares) and **Azo-DD-Tyr** (UV) (red circles) systems. **B)** Stern-Volmer plot of the fluorescence quenching of the **Azo-LD-Tyr** (no UV)-HSA (black squares) and **Azo-LD-Tyr** (UV) (red circles) systems.

The linear behavior of the Stern-Volmer plots suggests that a single class of fluorophore-quencher takes part in the association process (Fig. S29).

Evidence for a static quenching mechanism was provided by calculating the bimolecular quenching rate constants of the complexed protein. As shown in Table S3, the k_q values were found to be in the order of 10^{13} M^{-1} s^{-1}. These values are much higher than the maximum diffusion collisional quenching rate of various quenchers with biopolymers whose limit is close to $\approx 2.0 \times 10^{10}$ M^{-1} s^{-1}, and thus unambiguously emphasize the static nature of the quenching encountered.[10]

Table S3. Stern-Volmer (K_{sv}) and bimolecular quenching rate constants (k_q) for **Azo-LL-Tyr** (UV/no UV), **Azo-DD-Tyr** (UV/no UV) and **Azo-LD-Tyr** (UV/no UV)-HSA systems.

	K_{sv} (M^{-1})	k_q (M^{-1} s^{-1})
Azo-LL-Tyr (no UV)	$(6.1 \pm 0.2) \times 10^4$	$(1.7 \pm 0.2) \times 10^{13}$
Azo-LL-Tyr (UV)	$(3.3 \pm 0.3) \times 10^4$	$(0.9 \pm 0.3) \times 10^{13}$
Azo-DD-Tyr (no UV)	$(5.0 \pm 0.3) \times 10^4$	$(1.4 \pm 0.3) \times 10^{13}$
Azo-DD-Tyr (UV)	$(3.1 \pm 0.2) \times 10^4$	$(0.9 \pm 0.2) \times 10^{13}$
Azo-LD-Tyr (no UV)	$(5.3 \pm 0.3) \times 10^4$	$(1.5 \pm 0.3) \times 10^{13}$
Azo-LD-Tyr (UV)	$(3.3 \pm 0.2) \times 10^4$	$(0.9 \pm 0.2) \times 10^{13}$

Modified Stern-Volmer equation

The changes occurring in the intrinsic fluorescence intensity of the protein upon complexation gave the opportunity to calculate the association constants and the number of binding sites. In order to accomplish this task the modified Stern-Volmer equation was used (Fig. S30-31):[10]

$$\frac{F_0}{(F_0 - F)} = \frac{1}{K_b f_a [Q]} + \frac{1}{f_a} \qquad (9)$$

where K_b is the association constant and f_a is the fraction of the fluorophore accessible to the quencher i.e. the number of binding sites.

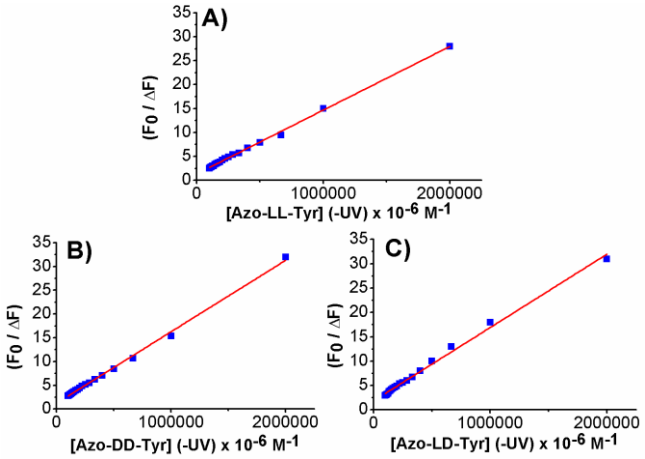

Figure S30. Modified Stern-Volmer plots of the **A) Azo-LL-Tyr** (no UV)-HSA, **B) Azo-DD-Tyr** (no UV)-HSA and **C) Azo-LD-Tyr** (no UV)-HSA association systems.

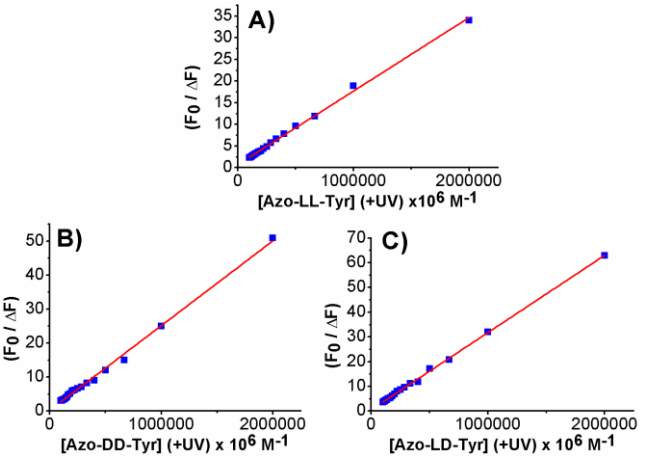

Figure S31. Modified Stern-Volmer plots of the **A) Azo-LL-Tyr** (UV)-HSA, **B) Azo-DD-Tyr** (UV)-HSA and **C) Azo-LD-Tyr** (UV)-HSA association systems.

The plot of $F_0/\Delta F$ *vs.* the inverse of the AB concentration is linear and provides the following values of association constant (K_b) and binding sites (f_a): **Azo-LL-Tyr** (no UV)-HSA: K_b: $(1.4 \pm 0.2) \times 10^5\ M^{-1}$ and f_a: 1.3; **Azo-DD-Tyr** (no UV)-HSA: K_b: $(6.8 \pm 0.4) \times 10^4\ M^{-1}$ and f_a: 1.2 **Azo-LD-Tyr** (no UV)-HSA: K_b: $(9.3 \pm 0.2) \times 10^4\ M^{-1}$ and f_a: 1.4; **Azo-LL-Tyr** (UV)-HSA: K_b: $(3.5 \pm 0.2) \times 10^4\ M^{-1}$ and f_a: 0.9; **Azo-DD-Tyr** (UV)-HSA: K_b: $(1.1 \pm 0.3) \times 10^4\ M^{-1}$ and f_a: 0.8; **Azo-LD-Tyr** (UV)-HSA: K_b: $(1.7 \pm 0.2) \times 10^4\ M^{-1}$ and f_a: 0.8. These values are in good agreement with those calculated by absorption spectroscopy.

Förster resonance energy transfer (FRET)

The absorption spectrum of **Azo-LL-Tyr** (UV/no UV), **Azo-DD-Tyr** (UV/no UV) and **Azo-LD-Tyr** (UV/no UV) overlap with the emission spectrum of HSA suggesting the existence of energy transfer (FRET) from Trp-214 (donor) to the photoswitches (acceptor) (Fig. S32-33). Briefly, we first calculated the J integral for each photochrome (UV/no UV)-HSA system by using the equation:[10]

$$J(\lambda) = \frac{\int_0^\infty F_D(\lambda)\varepsilon_A(\lambda)\lambda^4 d\lambda}{\int_0^\infty F_D(\lambda)d\lambda} \qquad (10)$$

where $F_D(\lambda)$ is the corrected fluorescence intensity of the Trp-214 residue in the wavelength range from λ to $\lambda + \Delta\lambda$ and $\varepsilon(\lambda)$ is the extinction coefficient of the acceptor at each λ.

The calculated values were then used to estimate the critical energy transfer distance defined as:[10]

$$R_0^6 = 8.79 \times 10^{-25} K^2 n^{-4} \Phi J \qquad (11)$$

where K_2 is the orientation factor related to the geometry of the donor and acceptor dipoles in random orientation and its values is taken as 2/3, n is the average refractive index of the media and φ is the fluorescence quantum yield of the donor (φ_{HSA}: 0.118).[12]

Finally, we determined the average distance between the D and the A (r) and the relative efficiency of transfer (E) from the difference in the emission profile of each HSA-photochrome system according to the following equation:[10]

$$E = 1 - \frac{F}{F_0} = \frac{R_0^6}{R_0^6 + r^6} \quad (12)$$

The calculated parameters are reported in Table S4.

Table S4. Overlap integral (J), critical distance (R_0), efficiency of energy transfer (E), average D-A distance (r) and rate constant of energy transfer (k_{ET}) calculated according to the FRET theory.

	J ($\times 10^{-14}$ cm^3 M^{-1})	R_0 (nm)	E	r (nm)	k_{ET} ($\times 10^7$ s^{-1})
Azo-LL-Tyr (no UV)	1.87	2.72	0.24	3.39	7.56
Azo-LL-Tyr (UV)	0.78	2.35	0.18	3.16	4.79
Azo-DD-Tyr (no UV)	1.26	2.54	0.22	3.20	7.08
Azo-DD-Tyr (UV)	0.73	2.33	0.19	3.07	5.41
Azo-LD-Tyr (no UV)	1.81	2.71	0.21	3.48	6.32
Azo-LD-Tyr (UV)	0.66	2.29	0.15	3.23	3.60

According to the FRET theory the rate of energy transfer can be calculated by using the following equation:[10]

$$k_{ET} = \tau^{-1} \times \left(\frac{R_0}{r}\right)^6 \quad (13)$$

where τ_{HSA} = 3.53 ns.[11] The derived values reported in Table S4 indicate that the non-radiative energy transfer can efficiently compete with the radiative deactivation of the tryptophan residue.

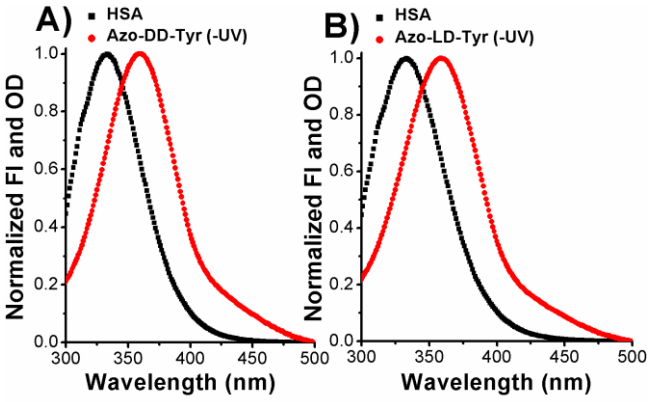

Figure S32. Overlap between the HSA emission spectrum and **A) Azo-DD-Tyr** (no UV) and **B) Azo-LD-Tyr** (no UV) absorption spectrum. r: [HSA] / [**Azo-DD-Tyr** or **Azo-LD-Tyr**] (no UV)] = 1.

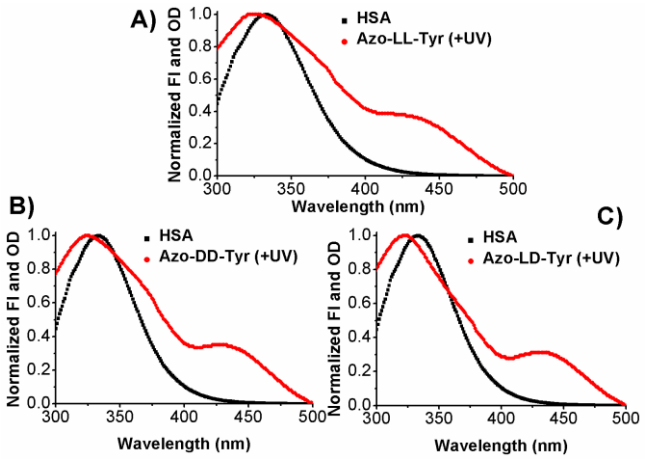

Figure S33. Overlap between the HSA emission spectrum and **A) Azo-LL-Tyr** (UV), **B) Azo-DD-Tyr** (UV) and **C) Azo-LD-Tyr** (UV) absorption spectrum. r: [HSA] / [**Azo-LL-Tyr** or **Azo-DD-Tyr** or **Azo-LD-Tyr**] (UV)] = 1.

Site-marker experiments

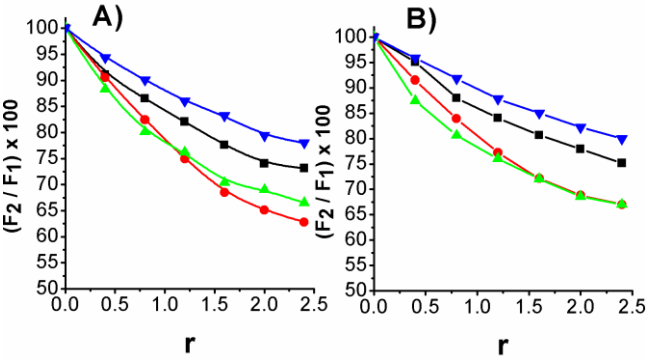

Figure S34. A) Plot of the fluorescent site-markers displacement assay. Blue curve: **Azo-DD-Tyr** (UV)-HSA-Warfarin; black curve: **Azo-DD-Tyr** (no UV)-HSA-Digitoxin; red curve: **Azo-DD-Tyr** (no UV)-HSA-Warfarin and green curve: **Azo-DD-Tyr** (UV)-HSA-Digitoxin. **B)** Blue curve: **Azo-LD-Tyr** (UV)-HSA-Warfarin; black curve: **Azo-LD-Tyr** (no UV)-HSA-Digitoxin; red curve: **Azo-LD-Tyr** (no UV)-HSA-Warfarin and green curve: **Azo-LD-Tyr** (UV)-HSA-Digitoxin. F_1 and F_2 are the fluorescence intensities of HSA-drugs in the absence and presence either of **Azo-DD-Tyr** or **Azo-LD-Tyr** (UV/no UV), respectively, at different molar ratios.

CD spectra of the photochromes

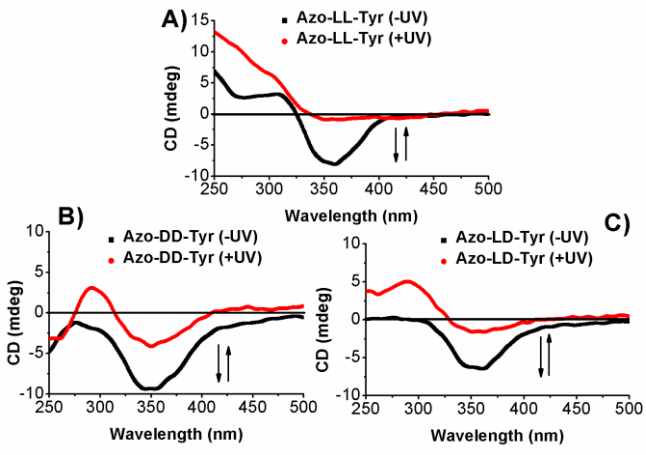

Figure S35. CD spectra for **A) Azo-LL-Tyr** (UV/no UV), **B) Azo-DD-Tyr** (UV/no UV) and **C) Azo-LD-Tyr** (UV/no UV).

CD spectra for Azo-DD-Tyr (UV) and Azo-LD-Tyr (UV)-HSA systems

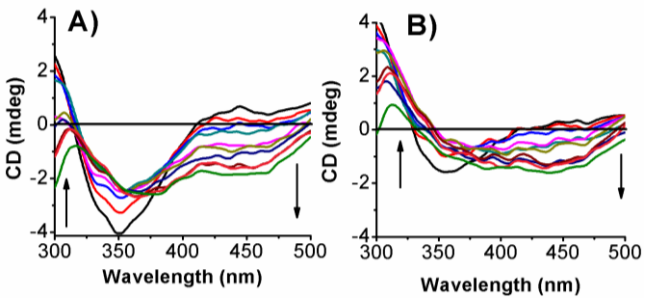

Figure S36. CD spectral change of **A) Azo-DD-Tyr** (UV) and **B) Azo-LD-Tyr** (UV) in the presence of incremental addition of HSA (0-50 μM).

HSA structural components

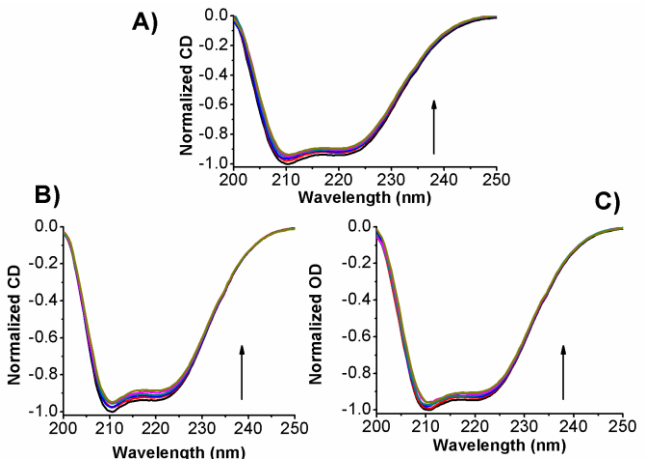

Figure S37. CD spectra of HSA in its free state and complexed form by **A) Azo-LL-Tyr** (no UV), **B) Azo-DD-Tyr** (no UV) and **C) Azo-LD-Tyr** (no UV). [HSA] 1 μM. r = 2, 4, 6, 8 and 10.

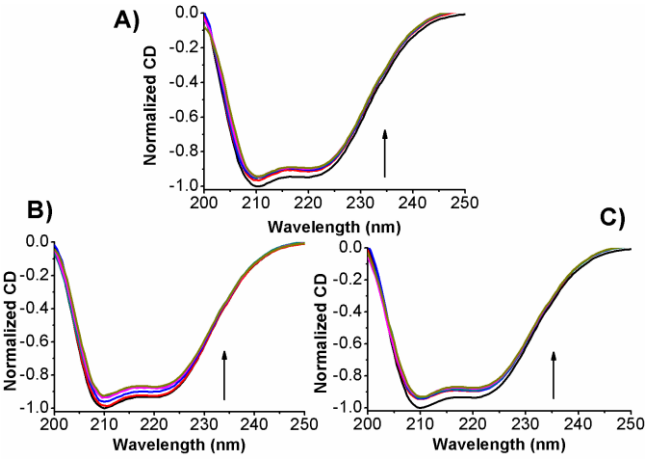

Figure S38. CD spectra of HSA in its free state and complexed form by **A) Azo-LL-Tyr** (UV), **B) Azo-DD-Tyr** (UV) and **C) Azo-LD-Tyr** (UV). [HSA] 1 μM. r = 2, 4, 6, 8 and 10.

Table S5. Secondary structure variations of the native HSA upon complexation with the photochromes at different molar ratios (r). r = [Photochrome (UV/no UV)] / [HSA free].

	α-helix (%)	β-sheet (%)	
HSA (free)	64.18	7.30	r = 0
Azo-LL-Tyr (no UV)	63.54	7.51	r = 2
Azo-LL-Tyr (no UV)	62.67	7.66	r = 4
Azo-LL-Tyr (no UV)	61.59	8.06	r = 6
Azo-LL-Tyr (no UV)	60.74	8.36	r = 8
Azo-LL-Tyr (no UV)	59.89	8.55	r = 10

Azo-LL-Tyr (UV)	60.38	8.10	r = 2
Azo-LL-Tyr (UV)	59.63	8.42	r = 4
Azo-LL-Tyr (UV)	59.45	8.85	r = 6
Azo-LL-Tyr (UV)	58.75	8.95	r = 8
Azo-LL-Tyr (UV)	57.93	9.21	r = 10
Azo-DD-Tyr (no UV)	64.01	7.35	r = 2
Azo-DD-Tyr (no UV)	63.93	7.37	r = 4
Azo-DD-Tyr (no UV)	63.86	7.43	r = 6
Azo-DD-Tyr (no UV)	63.72	7.49	r = 8
Azo-DD-Tyr (no UV)	63.63	7.53	r = 10
Azo-DD-Tyr (UV)	63.6	7.46	r = 2
Azo-DD-Tyr (UV)	62.8	7.58	r = 4
Azo-DD-Tyr (UV)	62.3	7.62	r = 6
Azo-DD-Tyr (UV)	61.9	7.74	r = 8
Azo-DD-Tyr (UV)	61.7	7.99	r = 10
Azo-LD-Tyr (no UV)	64.07	7.36	r = 2
Azo-LD-Tyr (no UV)	63.93	7.42	r = 4
Azo-LD-Tyr (no UV)	63.35	7.45	r = 6
Azo-LD-Tyr (no UV)	63.08	7.47	r = 8
Azo-LD-Tyr (no UV)	63.01	7.47	r = 10
Azo-LD-Tyr (UV)	60.55	8.43	r = 2
Azo-LD-Tyr (UV)	59.63	8.63	r = 4
Azo-LD-Tyr (UV)	59.32	8.83	r = 6
Azo-LD-Tyr (UV)	59.12	8.84	r = 8
Azo-LD-Tyr (UV)	53.87	9.11	r = 10

References

1. A. Venancio-Marques, A. Bergen, C. Rossi-Gendron, S. Rudiuk and D. Baigl, *ACS Nano*, 2014, **8**, 3654-3663; M. Deiana, Z. Pokladek, K. Matczyszyn, P. Mlynarz, M. Buckle and M. Samoc, *J. Mater. Chem. B*, 2017, **5**, 1028.
2. Gaussian 09, Revision E.01, M. J. Frisch, G. W. Trucks, H. B. Schlegel, G. E. Scuseria, M. A. Robb, J. R. Cheeseman, G. Scalmani, V. Barone, B. Mennucci, G. A. Petersson, H. Nakatsuji, M. Caricato, X. Li, H. P. Hratchian, A. F. Izmaylov, J. Bloino, G. Zheng, J. L. Sonnenberg, M. Hada, M. Ehara, K. Toyota, R. Fukuda, J. Hasegawa, M. Ishida, T. Nakajima, Y. Honda, O. Kitao, H. Nakai, T. Vreven, J. A. Montgomery, Jr., J. E. Peralta, F. Ogliaro, M. Bearpark, J. J. Heyd, E. Brothers, K. N. Kudin, V. N. Staroverov, R. Kobayashi, J. Normand, K. Raghavachari, A. Rendell, J.

C. Burant, S. S. Iyengar, J. Tomasi, M. Cossi, N. Rega, J. M. Millam, M. Klene, J. E. Knox, J. B. Cross, V. Bakken, C. Adamo, J. Jaramillo, R. Gomperts, R. E. Stratmann, O. Yazyev, A. J. Austin, R. Cammi, C. Pomelli, J. W. Ochterski, R. L. Martin, K. Morokuma, V. G. Zakrzewski, G. A. Voth, P. Salvador, J. J. Dannenberg, S. Dapprich, A. D. Daniels, Ö. Farkas, J. B. Foresman, J. V. Ortiz, J. Cioslowski, and D. J. Fox, Gaussian, Inc., Wallingford CT, 2009.

3. A. D. Becke, *J. Chem. Phys.* 1993, **98**, 1372-1377.
4. M. Deiana, Z. Pokladek, M. Ziemianek, N. Tarnowicz, P. Mlynarz, M. Samoc and K. Matczyszyn, *RSC Adv.*, 2017, **7**, 5912.
5. C. Louis-Jeune, M. A. Andrade-Navarro and C. Perez-Iratxeta, *Proteins*, 2012, **80**, 374-381; N. J. Greenfield, *Nat. Protoc.*, 2006, **1**, 2876.
6. Y. –J. Hu, Y. Liu and X. –H. Xiao, *Biomacromolecules*, 2009, **10**, 517-521.
7. H. A. Benesi and J. H. Hildebrand, *J. Am. Chem. Soc.*, 1949, **71**, 2703; M. Deiana, B. Mettra, K. Matczyszyn, D. Pitrat, J. Olesiak-Banska, C. Monnereau, C. Andraud and M. Samoc, *Biomacromolecules*, 2016, **17**, 3609; M. Deiana, B. Mettra, K. Matczyszyn, K. Piela, D. Pitrat, J. Olesiak-Banska, C. Monnereau, C. Andraud and M. Samoc, *Phys. Chem. Chem. Phys.*, 2015, **17**, 30318; M. Deiana, K. Matczyszyn, J. Massin, J. Olesiak-Banska, C. Andraud and M. Samoc, *PLoS ONE*, 2015, **10**, e0129817.
8. A. A. Sabouri and A. A. Moosavimovahedi, *Biochem. Educ.*, 1994, **22**, 48.
9. B. Dumat, G. Bordeau, E. Faurel-Paul, F. Mahuteau-Betzer, N. Saettel, G. Metge, C. Fiorini-Debuisschert, F. Charra and M. -P Teulade-Fichou, *J. Am. Chem. Soc.*, 2013, **135**, 12697; R. Kakkar and R. G. Suruchi, *J. Mol. Struc-Theochem.*, 2002, **579**, 109.
10. J. R. Lakowicz, Principles of Fluorescence Spectroscopy, Springer, New York, 3rd edn, 2006; M. Deiana, B. Mettra, L. M. Mazur, C. Andraud, M. Samoc, C. Monnereau and K. Matczyszyn, ACS Omega, 2017, DOI: 10.1021/acsomega.7b00665.
11. M. El-Kemary, M. Gil and A. Douhal, *J. Med. Chem.*, 2007, **50**, 2896.
12. A. Sytnik and I. Litvinyuk, *Proc. Natl. Acad. Sci. U. S. A.*, 1996, **93**, 12959.